



university of
 groningen

faculty of science
 and engineering

kapteyn astronomical
 institute

BACHELOR RESEARCH PROJECT

Predicting the Near-Earth Object harvest of the BlackGEM Telescope Array

Jasper Jacob POSTEMA
s3164063

Supervised by:
K. FRANTSEVA
dr. G. A. VERDOES KLEIJN

July 5, 2019

Abstract

The BlackGEM telescope array's main goal is to detect the optical counterparts of gravitational waves, but its surveys could also be used to detect Near-Earth Objects, NEOs. Using a simulation of one of BlackGEM's operations, it is shown that it is possible to (re)detect known NEOs with the BlackGEM telescopes. Furthermore it is determined that one of BlackGEM's surveys, the Southern All Sky Survey, SASS, has no bias in observing NEOs. This means that NEOs observed by the SASS are an accurate representation of the total NEO population. This allowed us to determine that the predicted amount of detected previously unknown NEOs is 4244. Most of these newly discovered NEOs have a diameter around 200 m. This is an interesting size, because there are still unknown Potentially Hazardous Objects, PHOs, around those sizes. Since the pointing schedule of the real SASS will most likely not be the same as the pointing schedule of the simulated SASS, the exact amount of (re)detections and previously unknown discoveries will most likely not be the same for the real SASS. However, because the real SASS will survey the same population in the same part of the sky, it is likely that the amount of detections done by the real survey is similar to the amount of detections done by the simulated survey. We can therefore conclude that the BlackGEM telescope array can be used to (re)detect known NEOs and discover currently unknown NEOs.

Abbreviations

FSS Fast Synoptic Survey

GW Gravitational Wave

LTS Local Transient Survey

MAB Main Asteroid Belt

MPC Minor Planet Center

NEO Near-Earth Object

PHO Potentially Hazardous Object

S/N Signal to Noise

SASS Southern All Sky Survey

Contents

1	Introduction	5
1.1	Asteroids	5
1.1.1	Near-Earth Objects	7
1.2	History of asteroid surveys	8
1.3	Recent asteroid surveys	9
1.4	What is the BlackGEM telescope array?	11
1.5	Goal of the research	12
2	The BlackGEM telescope array	13
2.1	Telescopes and bands	13
2.2	Limiting magnitude	14
2.3	BlackGEM observational campaigns	15
3	Detection rules for NEOs	18
3.1	Absolute magnitude (H)	18
3.2	Albedo	19
3.3	The Slope parameter (G)	21
3.4	The Minor Planet Center	21
3.5	Trailing loss	22
4	Simulation	23
4.1	The Sky Body Tracker project	23
4.2	Fields of the SASS	25
4.3	The calculations	28
4.3.1	Assumptions in the simulation.	28
4.3.2	Calculating a detection	29
5	Results	33
5.1	interpreting results	33
5.2	NEOs detection count	33
5.3	Detection fractions	33
5.4	BlackGEM bias	35

5.5	Unknown asteroid detections	35
6	Discussion	38
6.1	Assumptions	38
6.2	Code improvements	39
6.3	Further research	39
7	Conclusion	41
8	Appendix A: detection fractions as a function of diameter in each Black-GEM band	42
9	Appendix B: Problems, solutions and possible improvements	44
10	Appendix C: SASS simulation code	45

1 Introduction

1.1 Asteroids

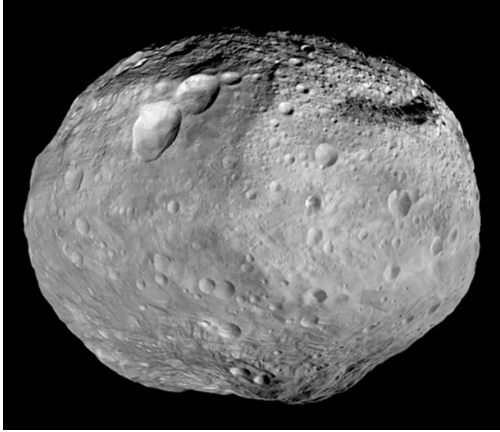


Figure 1: Image of the Main Belt Asteroid (4) Vesta, the second largest known asteroid. Taken by the Dawn spacecraft. (Courtesy: NASA/JPL)

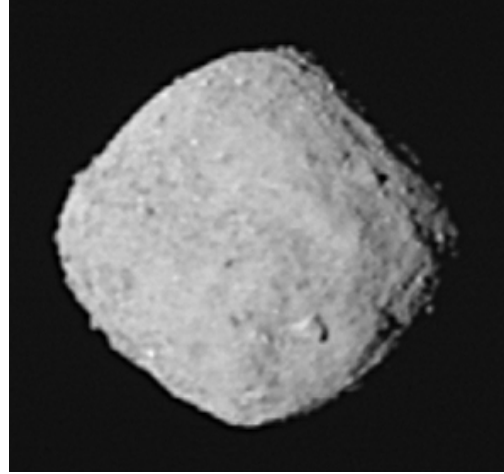


Figure 2: Image of the potentially hazardous object Bennu, the image consists of 12 images taken by OSIRIS-REx. (Courtesy: NASA)

The formation of asteroids begins in the early days of the Solar System. During this time, about 4.6 million years ago (Bouvier and Wadhwa, 2010), the Solar System consisted of the Sun surrounded by a protoplanetary disk. A protoplanetary disk is a disk made solely of gas and dust. Planetesimals are clusters of matter that can turn into planets by accreting more matter, planetesimals were initially formed from the materials in the protoplanetary disk. Some planetesimals became larger than 100 km in diameter, so their cores became hotter than 1600 K and started to melt (Moskovitz and Gaidos, 2011). This leads to differentiation, which means that the heavier elements sink to the centre of the planetesimal forming the iron core, while the outside remains rocky. Asteroids come in different types based on composition. Therefore, not all asteroids have the same colour and material. Some asteroids are more rocky or even iron, while others are icy or carbonaceous. The different types of asteroids are denoted by letters. C types are the most common with 40% of all asteroids being part of this class. 30 to 35 % of all asteroids are S types, which makes this the second most common type. The third most common types are D and P types, they both only contain 5 to 10 % of all asteroids (de Pater and Lissauer, 2015), in the thesis we will only focus on the two most common types, C and S type asteroids. The planets all formed around the same time, about 100 million years after the Sun. However, no planets would form between Mars and Jupiter. Only small objects would remain, the asteroids. The group of asteroids in the region between Mars and Jupiter is called the Main Asteroid Belt, MAB. The reason why planets had not formed in orbits between Mars and

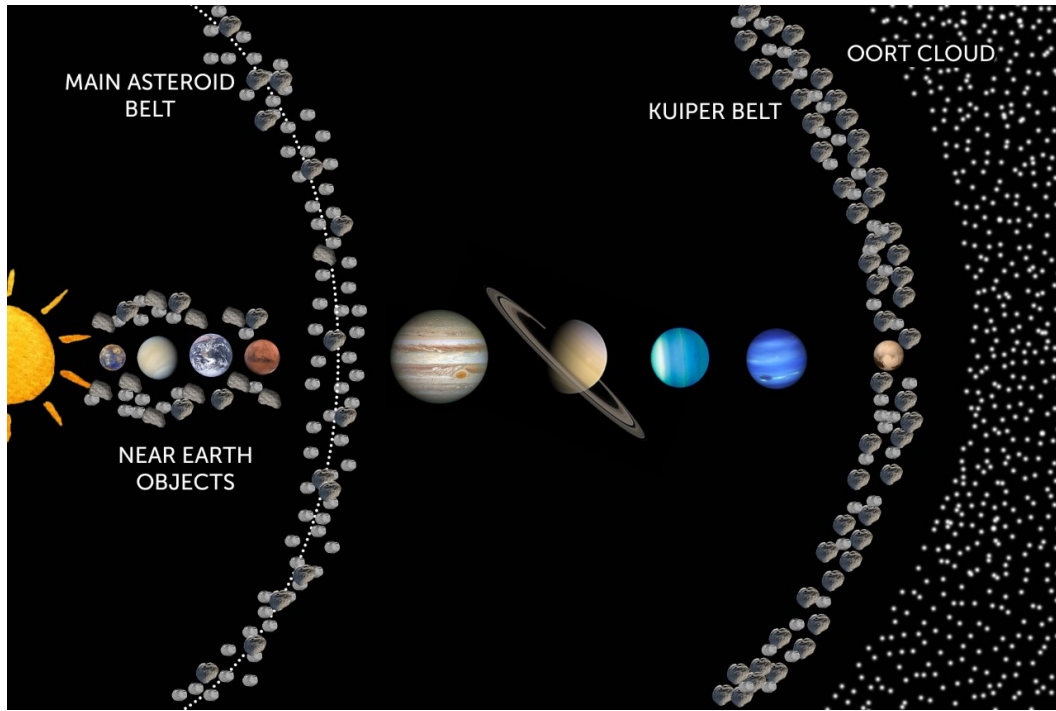


Figure 3: Artist rendition of the Solar System with some of its minor body populations. (Courtesy: Kateryna Frantseva)

Jupiter is due to Jupiter's gravity, or more specifically due to orbital resonances. Orbital resonances occur when multiple bodies rotate around a common centre of mass and their orbital periods are related by a ratio small integers. Because a planetesimal and Jupiter both orbit around the Sun, there are times when Jupiter is close to the planetesimal and times when Jupiter is further away. This means that there are times that the gravitational effect of Jupiter on the planetesimal is strong and times that the gravitational effect is weak. This happens at a regular pace. Depending on the pace, this could either strengthen or weaken the orbit of the planetesimal. Strengthening an orbit means that the orbital parameters of the planetesimal are kept from changing, so the orbit remains the same for a long time. Weakening an orbit means that the eccentricity and the inclination of the planetesimal is increased, so that the planetesimal gets a more elliptical orbit and can interact with other planets, which changes its orbit even more. This effect is called orbital resonance. Many of the planetesimals between Mars and Jupiter were ejected due to resonances, but the ones in the MAB were in a stable orbit, so they remained.

Objects between Mars and Jupiter are called asteroids in the MAB. Most of the asteroids that we see now have undergone no significant transformation after they were created as planetesimal. If a planetesimal would not grow large enough to differentiate it would remain stony and therefore also create stony asteroids when broken up. If a planetesimal would however grow larger, become differentiated and break up due to collisions, other types of

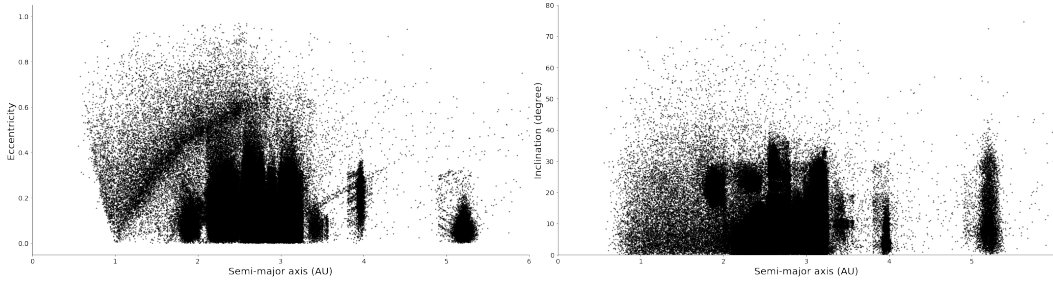


Figure 4: Eccentricity and inclination versus the semi-major axis of all known asteroids with a semi-major axis less than or equal to 6 AU. A grouping of asteroid families due to orbital parameters can clearly be seen.

asteroids would be created. Asteroids made of the interior of the big planetesimal could be completely metallic, due to the differentiated core. Asteroids made of the outside would still be stony, but combinations of the two also occur. As of 3 July 2019, there are 795996 known asteroids, with diameters ranging from tens of meters to hundreds of kilometers. Fig. 4 shows the eccentricity and inclination of asteroids with a semi-major axis smaller than or equal to 6 AU. From this figure, we can clearly see that there are some groups of asteroids depending on their orbital parameters. These groups are called families.

Some planetesimals remained largely intact throughout their lives, an example is the dwarf planet Ceres in the MAB. Besides asteroids, comets can also form from planetesimals. Comets and asteroids are very similar in their sizes and shapes, however there are also differences between the two objects. Asteroids are made of stony or even metallic materials while comets are more icy, this is because comets formed further away from the Sun than asteroids. Comets often also have an orbit that is way more elliptic than an asteroids orbit. But their main difference is that comets can form a tail when exposed to solar radiation, this is due to their more icy interior. A reason why it might be interesting to study asteroids, is because they contain information about the formation of the Solar System, because parts of some asteroids have been unaltered since the start. Since this has to do with the material of the asteroid, this can only be studied when a meteorite is found on Earth or when a piece of the asteroid is brought from space back to Earth.

1.1.1 Near-Earth Objects

Small bodies in the Solar System are gravitationally influenced by the planets, this can repel the small bodies from their orbit. If their orbit gets perturbed a small amount due to a collision or some other cause, they might get into an unstable orbit and be expelled from their population. This however does not mean that the asteroid leaves the Solar System, they can get gravitationally attracted to another, less populated, stable orbital populations. Take for instance the Mars crossers. These asteroids orbit the Sun in such a way that their orbit crosses the orbit of Mars. Another example is the Trojan asteroids. These move around the Sun in the same orbit as Jupiter, so they form clumps in front and behind the

planet's path.

Even though these clusters are very interesting, because there is still so much to learn, in this thesis we will focus on the near-Earth Object, NEO, population. It is therefore useful to first explain precisely what NEOs are. NEOs include all objects (asteroids and comets) with a perihelion¹ distance less than 1.3 AU (NEO). As of 3 July 2019, there are 20073 NEOs discovered. Their orbital parameters can be seen in figure 4, where their population is contained in the V-shape around 1 AU in the eccentricity plot. The NEOs are in a V-shape, because a minor body with a larger semi-major axis must have a larger eccentricity to still be qualified as a NEO. The orbital parameters of NEOs are quite different from the orbital parameters of the MAB asteroids. The difference lies in the fact that NEOs can not have a high semi-major axis without having a large eccentricity, so the NEO population is distributed differently than the MAB population in Fig. 4.

There are different types of NEOs, based on the properties of their orbits. Based on the orbital parameters there are 4 groups of NEOs such as the Atiras, the Atens, the Appollos and the Amors. The first family of NEOs is the Atiras which orbits are entirely contained inside Earth's orbit. There are 20 known Atiras as of 3 July 2019. The second family of NEOs is the Atens, whose orbits cross the Earth's orbit but have a semi-major axis smaller than the Earth's. There are 1507 known Atens as of 3 July 2019. The third family of NEOs is the Appollos, that are also Earth crossers, but with a semi-major axis larger than the Earth's. There are 10987 Appollos known as of 3 July 2019. Finally there are the Amors, with orbits outside the Earth's orbit but still have a perhelion distance of less than 1.3 AU. There are 7530 Amors known as of 3 July 2019.

Part of the NEO population are considered to be Potentially Hazardous objects, PHOs. These asteroids and comets have a diameter of at least 140 meter and come within a distance of 0.05 AU to the Earth and therefore have a chance to collide with the Earth. There are 1965 known PHOs as of 3 July 2019. It is useful to study PHOs, because they might some day collide with the Earth and it would be useful to know when that will happen. Another reason why NEOs are interesting to study, is because it might be possible for a space mission to visit one such object.

As said before, asteroids provide knowledge about the early Solar System, so getting information about the orbit of those asteroids close to home might allow future space missions to send a lander to an asteroid to get information about the interior, unaltered by the Earth.

1.2 History of asteroid surveys

The different minor body populations are only known, because they have been discovered by the many asteroid surveys that were preformed. Asteroids have always been a topic of great interest to astronomers. The very first asteroid, Ceres, was discovered by Giuseppe Piazzi in 1801 (Cer). Asteroids then were detected by observing the sky for multiple nights,

¹The perihelion is the point in the orbit that is nearest to the Sun.

looking for "stars" that moved across the sky and could not be attributed to known planets. During most of the 19th century, before photographic astronomy, only 447 (Jedicke, Granvik, Micheli, Ryan, T., and Yeomans, 2015) asteroids were detected this way. This is of course because astronomers were limited by their eyesight. After the invention of photographic astronomy, photographic plates could be used to detect moving objects in front of a static background by comparing images of the sky that were taken several minutes apart. Using this higher tech, many more asteroids were detected (Jedicke et al., 2015). From 1984 onward, CCD chips were used in telescopes. This allowed for even sharper and deeper images of the sky. The amount of discovered asteroids increased therefore even faster. Not only could we find the biggest and closest of asteroids, but smaller and further ones also became known. In Fig. 5 the number of discovered asteroids in a decade is shown as a function of the decade (Jedicke et al., 2015).

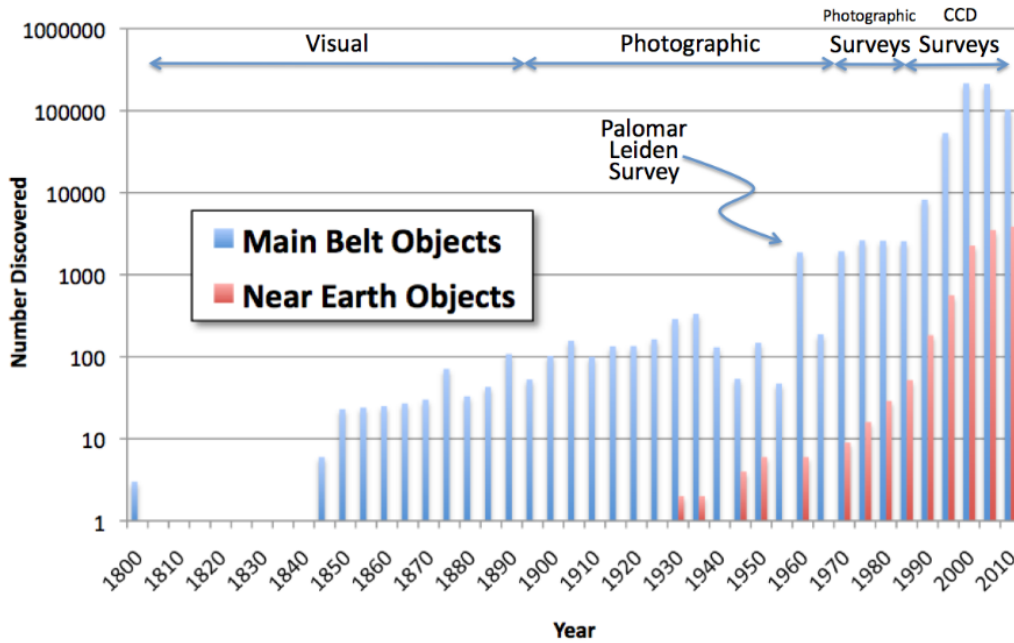


Figure 5: Number of asteroid discoveries per decade as a function of decade since the first discovery. The Palomar Leiden Survey is shown, because it was very much ahead of its time. Picture credit: Surveys, Astrometric Follow-up & Population Statistics (Jedicke et al., 2015).

1.3 Recent asteroid surveys

A few recent surveys will be discussed now. The Lincoln Near-Earth Asteroid Research program (LINEAR) started in 1996 and ended in 2013 (Jedicke et al., 2015). The survey was performed from Socorro, New Mexico in the USA, which means that the Northern sky was observed. The CCDs of this survey allowed for quick measurements, and large parts of the sky could be observed each night. LINEAR could measure asteroids down to a visual

apparent magnitude of 19. A larger apparent magnitude means a less visible object, so LINEAR can detect asteroids that are brighter than an apparent magnitude of 19. The magnitude system will be explained in more detail in Section 3. This survey discovered more than one third of all NEOs with a diameter of 1 km or larger, which comes down to about 300 NEOs (Harris and D'Abramo, 2015).

A more modern survey that started in 2010 is the Panoramic Survey Telescope and Rapid Response System, Pan-STARRS, which is still operating today (Jedicke et al., 2015). It is operating from the island Haleakala in the USA, and therefore observes the Northern sky as well. In 2018 it discovered 30 % of all newly discovered asteroids that year (NAS). The survey can measure down to a visual apparent magnitude of 22, which is the best sensitivity achieved by an asteroid survey so far. This means that the survey can measure fainter objects than has ever been done before. Another benefit of Pan-STARRS is that its position allows for it to detect PHOs near the Sun, which is where the density is largest. This has been confirmed by observations and models (Vereš, Jedicke, Wainscoat, Granvik, Chesley, Abe, Denneau, and Grav, 2009).

The most prominent survey planned right now is the Large Synoptic Survey Telescope, LSST. LSST will start its scientific operations in 2022 and continue for as long as possible. There are many applications to the result of the survey (LSST Science Collaboration, Abell, Allison, Anderson, Andrew, Angel, Armus, Arnett, Asztalos, and Axelrod, 2009). For instance, mapping the dust in the Milky Way, finding stars in nearby galaxies or investigate large scale structure. There are also plans to discover and rediscover asteroids down to an apparent magnitude of 24.7. This survey will be very important to the field of asteroid astronomy, because it will be able to detect fainter asteroids than ever before and because it will preform on the Southern hemisphere, where few surveys have taken place.

NEOs were always and still are easier to detect than asteroids in other parts of the Solar System. This is because asteroids closer to the Earth seem to move faster across the sky than asteroids further away. So throughout the history of asteroid astronomy, the same technique has always been used. A piece of the sky is observed for a certain amount of time and the objects that change position are observed asteroids. Two things that changed over time is the accuracy and precision of the measurements, which would of course yield more detections.

In 1998 NASA set a goal to discover 90 % of all NEOs larger than 1 km. In 2005 this goal got extended so that 90 % of all NEOs larger than 140 m were to be discovered (George E. Brown, Jr. Near-Earth Object Survey Act (PHO)). Because of this, at least 23000 NEOs with a diameter larger than 140 m have been discovered (Jedicke et al., 2015). The limit was put at 140 m, because PHOs are defined to be larger than 140 m. However there are still some gaps in our knowledge about minor bodies in general. For instance most surveys were preformed on the Northern Hemisphere (Jedicke et al., 2015). The Northern and Southern sky are not the same, so we know less about NEOs that are predominantly in the Southern sky. We also know less about very small and therefore faint asteroids. New surveys that search unexplored skies for faint sources will therefore always be useful in the field of asteroid astronomy.

1.4 What is the BlackGEM telescope array?

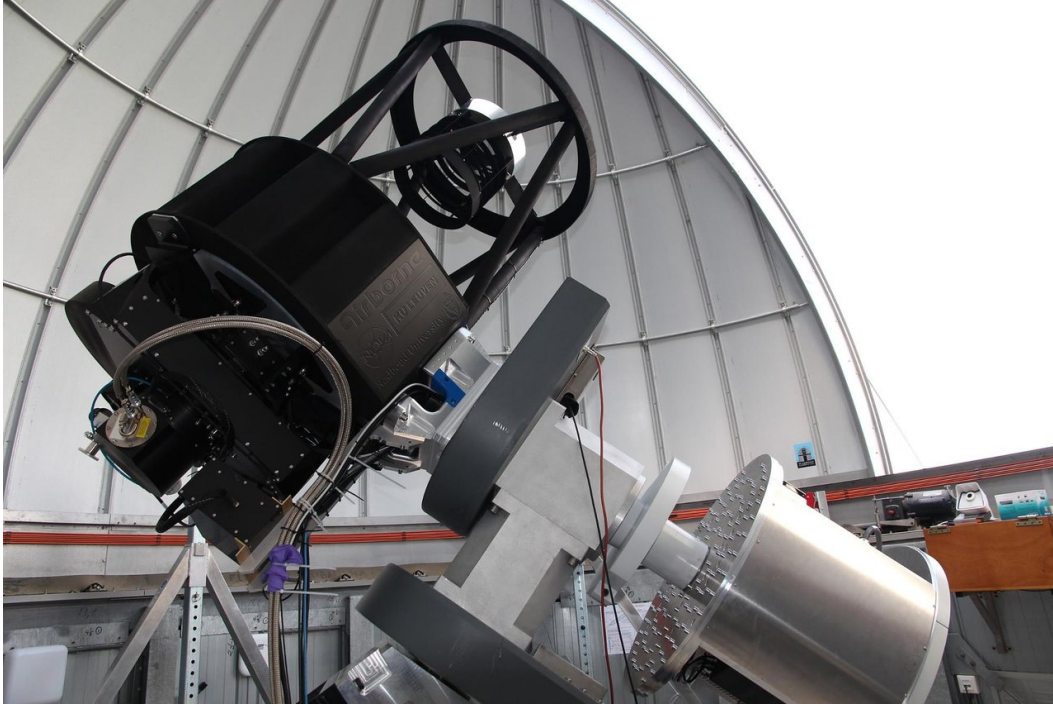


Figure 6: One telescope of the BlackGEM telescope array (Courtesy of S. Bloemen).

Since the current catalogues of minor bodies are incomplete, there is need for more asteroid surveys. We will discuss the BlackGEM telescope array, which will be used to survey the sky. BlackGEM is a wide-field telescope array built by among others NOVA (Netherlands Research School for Astronomy) (Bla, b). BlackGEM starts with 3 telescopes, which will possibly be upgraded to 15, each with a diameter of 65 cm, located in La Silla in Chile. This location is chosen because of the good weather, between 1984 and 2017, 61 % of the nights were great for observations (LaS). To compare, in Groningen in 2018, about 80 % of the days were cloudy (Gro). The seeing in La Silla is as great as its weather. Seeing is created by turbulence in the atmosphere and bad seeing causes the Stars' position in the sky to be ill-determined or causes stars twinkle. The seeing at La Silla is 0.9" median. The BlackGEM project has three main scientific objectives. Gravitational waves are disturbances of spacetime that travel with the speed of light and are emitted away when two massive objects (often black holes) merge. Since gravitational waves can not be detected by optical telescopes there is a need for other types of detectors. The Laser Interferometer Gravitational-Wave Observatory, LIGO for instance can detect gravitational waves. However in the case where a neutron star merges with a black hole, light is emitted as well. The first objective of BlackGEM is to detect and characterize this optical counterpart to gravitational wave mergers. The light from some sources in the sky may look like that of a gravitational wave merger. To be sure that a measurement actually corresponds to a

gravitational wave merger event, the second objective is to uncover the transients in the sky that may masquerade as gravitational wave counterparts. The final objective is to chart the population of gravitational wave progenitors: massive binary stars. To achieve these objectives, BlackGEM will measure the entire southern sky during a number of surveys.

1.5 Goal of the research

During the surveys, BlackGEM will take continuous pictures of the entire sky. As you might recall from the second section, this is also done during asteroid surveys. It could therefore be possible that asteroids can be detected using the data from the BlackGEM surveys. The objective of this thesis is to simulate the data from a BlackGEM survey and to find out which fraction of NEOs, depending on type, can be detected in the images of the survey.

2 The BlackGEM telescope array

As explained in the introduction, BlackGEM is a telescope array build with the intention of measuring the optical counterpart of gravitational waves, GWs. To help with this, BlackGEM performs four different observational campaigns with different priorities. Each campaign uses the same telescopes, which is why they cannot be performed at the same time.

2.1 Telescopes and bands

BlackGEM consists of three identical telescopes, each with a square field of view of 2.7 square degree. The CCD consists of a 10500 by 10500 pixel array with a $9\text{ }\mu\text{m}$ pixel size. This means that each pixel will correspond to a square with sides of $0.56''$ length. $1''$ is an arcsecond and is equal to $\frac{1}{3600}$ of a degree. The telescopes can look through one of 6 different filters (u,g,q,r,i,z), as shown in Fig. 7, at a time (Bla, a).

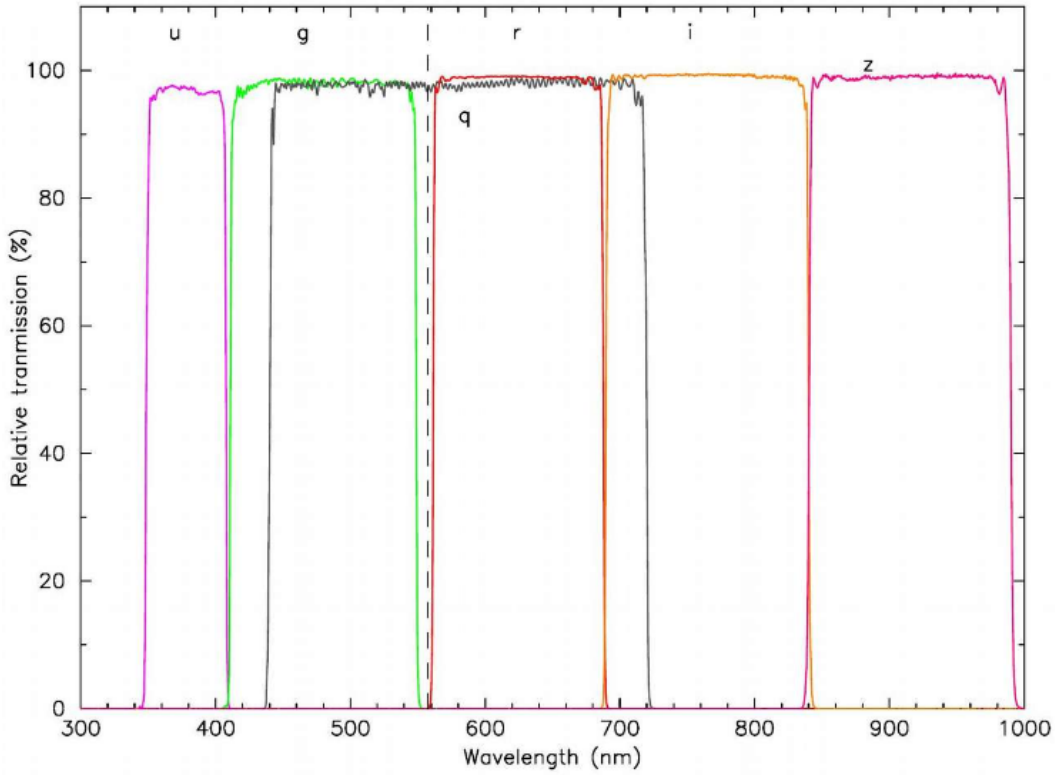


Figure 7: The different BlackGEM filters and their wavelengths. Image reproduced from Bla (a).

A filter is a thin film that can be put in front of the camera and only allows light in a

certain wavelength range to be passed through. In Fig. 7 it can be seen that transmission spikes steeply at the edges of the wavelength range for each filter. This is so that only light with wavelengths in the desired wavelength range will go through the filter. The wavelength range is called a band. So for instance, the u-band is approximately between 350 and 410 nm as can be seen in Fig. 7.

Band	Effective wavelength (\AA)	Bandwidth (\AA)
u	3800	600
g	4850	1400
q	5800	2800
r	6250	1220
i	7650	1500
z	9150	1500

Table 1: Effective wavelength and bandwidth of each BlackGEM band.

The effective wavelength of a filter is the wavelength in the middle of the band. In Table 1 the effective wavelength and width of each band is shown.

The q-band is the widest of the 6 bands. It is the most often used band during all of the BlackGEM surveys. This band is the most precise band of BlackGEM, it can detect objects fainter than any of the other bands. The brightness of an object is always dependent on the wavelength at which you look at the object. An object can for instance be very bright at an infrared wavelength, but very dim when you look at it at an ultraviolet wavelength. The absolute and apparent magnitude therefore also depend on the wavelength and with that the filter through which you look at the object. The absolute magnitude is a measure for how bright an object is and the apparent magnitude is a measure for how bright an object is perceived from Earth. It could therefore happen that an object is detected in a certain band, while it is invisible in another.

2.2 Limiting magnitude

Each band of the BlackGEM telescope has its own limiting magnitude. To understand the limiting magnitude, we need to look a bit deeper into what the CCD of a telescope detects. The CCD consists of an array of pixels and each pixel counts the amount of photons coming in. It does not discriminate between photons from a source, photons from the background or photons generated by noise. Noise is generated by for example the Moon, the instrument itself and even the stellar object, which is due to Poisson statistics of photon emission. This noise is unwanted, but often quite small. However if a source is faint, the noise could be a significant amount of the measured photon flux. The signal to noise, S/N, is the ratio between the photons from the source and the photons from the noise. For a faint source, this value will be smaller, so for a source with a larger magnitude, the S/N will be smaller. For BlackGEM, the magnitude for which the S/N is equal to 5 is defined as the limiting magnitude. If an object has an apparent magnitude larger than the limiting magnitude,

it does not mean that it will not be detected, but just that there is a reasonable chance that it might be confused for background noise. That also means that it is not fully certain that an object with an apparent magnitude smaller than the limiting magnitude will be detected. For the purposes of this thesis though it is sufficient to state that any object with an apparent magnitude larger than the limiting magnitude will not be detected, while an object with an apparent magnitude smaller than the limiting magnitude will always be detected. Because each filter is made differently and the sky does not generate the same noise in each band, the limiting magnitude is different for each band. The phase of the Moon also influences the limiting magnitude, since a full Moon is another unwanted source of light, which adds to the noise.

Band	New Moon	Full Moon
u	21.3	19.6
g	22.4	21.4
q	22.7	21.9
r	21.7	21.4
i	21.2	20.9
z	20.3	20.1

Table 2: The limiting magnitude of BlackGEM’s different bands for full and new Moon (P.Groot and S.Bloemen private communication).

The limiting magnitudes of the different bands for full and new Moon are shown in Table2.

The fact that the limiting magnitude is different in each BlackGEM band means that a certain object can be measured in one band but not in another. If an object’s apparent magnitude is larger than the limiting magnitude in one band, it can be smaller than the limiting magnitude in another band.

2.3 BlackGEM observational campaigns

BlackGEM operations will consist of four different surveys: the GW follow-up, the Local Transient Survey, LTS, the Fast Synoptic Survey, FSS, and the Southern All Sky Survey, SASS, in that order of priority.

Because the main objective of BlackGEM is to detect the optical counterparts of GWs, measuring these will have the highest priority. The campaign during which BlackGEM will search for the optical counterparts of GWs is called the GW follow-up. The measurements will be done when a trigger from GW observatories comes in. The radiative signals from GWs are extremely faint and their life time, the time before the signal fades away, is also very short. Because of this a background image of the entire southern sky needs to be created. If the brightness of the sky without a gravitational wave in all BlackGEM bands is very well known, a minor change from the background can be detected. The optical part of a GW is a minor change from the background, so using a very accurate background, the

optical counterparts of GWs can be detected. The SASS serves to create this background image.

The parts of the sky containing galaxies in the local universe are most interesting, because they can be used in the field of galactic astronomy as well. Since these parts are also needed to make a background of the whole sky, they might as well be measured first. These fields are addressed during the LTS, which has the second highest priority. A field is a square part of the sky with an area of 2.7 degrees, which is the field of view of a single telescope. During the LTS, BlackGEM will measure each field once in the u, q and i band. This makes sure that these interesting fields are well observed over a large frequency range.

The final two surveys have an equal, lowest, priority. The Fast Synoptic Survey (FSS) will look at one or two fields for an entire month in the u, q and i bands. The fields are measured for an entire month, so that quickly changing astronomical objects, like supernovae can be exposed. The survey will measure the fields in the u, q and i filter.

The SASS will survey all fields in the Southern sky once and measure 5 times in the 6 different BlackGEM bands. This is the main survey that will determine the background of the Southern sky. The filters have an integration time of 1 minute and an overhead time of 30 seconds. The overhead time is the time that it takes for the filters to switch between each other.

The LTS will be preformed 4 times per night for half an hour with 3 hour intervals. During the intervals, either the SASS or FSS will happen depending on the phase of the moon. During bright nights the FSS will be preformed and during dark nights, the SASS will be preformed. This is shown schematically in Fig. 8.



Figure 8: Schematic schedule of BlackGEM, where BG-LT is the Local Transient Survey, BG-SASS is the Southern All Sky Survey and BG-FSS is the Fast Synoptic Survey. Image reproduced from Bla (a).

Much of the information above was obtained using the BlackGEM website Bla (b).

We are trying to find out if any of the BlackGEM observational campaigns can be used to detect NEOs. The first step in this process is to determine which of the campaigns can be best used to find NEOs. One campaign we can ignore for certain is the GW follow-up.

The GW follow-up is only used when a gravitational wave is detected and can therefore not be used to reliable search for NEOs. Some relevant information about the remaining BlackGEM operations is shown in Table 3.

	LTS	FSS	SASS
Filters used	u, q and i	u, q and i	u, g, q, r, i and z
Area surveyed	Some parts	Whole Southern sky	Whole Southern sky
Time spend per field	depends on survey length	145 hours	45 minutes

Table 3: Some information about the BlackGEM surveys.

A NEO survey could have different objectives, it could for example be that the orbit of the NEOs should be determined, that the type of the NEOs should be determined or that NEOs with highly inclined orbits should be detected. Each survey has its own strengths, the LTS and FSS for example can very accurately determine the orbits of NEOs that move through their fields, because the fields are detected so often, the FSS and SASS can both be used to detect NEOs with any kind of orbit, because they survey the entire Southern sky and the SASS can determine the type of asteroid very well, because it detects in all of the BlackGEM bands. Another benefit of observing with the SASS is that it takes the least amount of time to complete the survey. For these reasons, we will determine how effective the SASS is at detecting NEOs. It is likely that the BlackGEM telescopes can contribute to the database of known NEOs, because the limiting magnitude of the BlackGEM bands is high enough to allow for asteroid detections. Since a significant amount of asteroids have an absolute magnitude higher than 20 and almost all asteroids with an absolute magnitude lower than 18 have already been detected (Harris and D’Abramo, 2015). This makes sure that the contribution of a NEO detection survey by BlackGEM could provide us with new asteroid detections. This is not unique for the SASS though.

3 Detection rules for NEOs

3.1 Absolute magnitude (H)

In order for someone to be able to detect an asteroid, the asteroid needs to be bright enough. Brightness of astronomical objects is measured in magnitudes. The magnitude of an object is a number that represents its brightness with respect to a certain reference object. A higher magnitude means a dimmer object and a lower magnitude means a brighter object. If an object is a hundred times as bright as another object, it means that its magnitude is 5 smaller than the other object, negative magnitudes are therefore also possible. There is also a difference between apparent and absolute magnitude. The apparent magnitude is the magnitude that an object has as viewed from Earth. This is also the magnitude that is seen by a telescope on Earth, for instance BlackGEM. If we can determine the apparent magnitude of an asteroid, we can determine if it can be observed by BlackGEM or not. The absolute magnitude of an object has different definitions, depending on the type of object. For asteroids, the absolute magnitude is denoted by H . Absolute magnitude, in the case of asteroids, is the apparent magnitude that the asteroid would have at 1 AU from the Earth and 1 AU from the Sun at zero solar phase angle. The phase angle is the angle between the light incident on the asteroid from the Sun and the light reflected by the object.

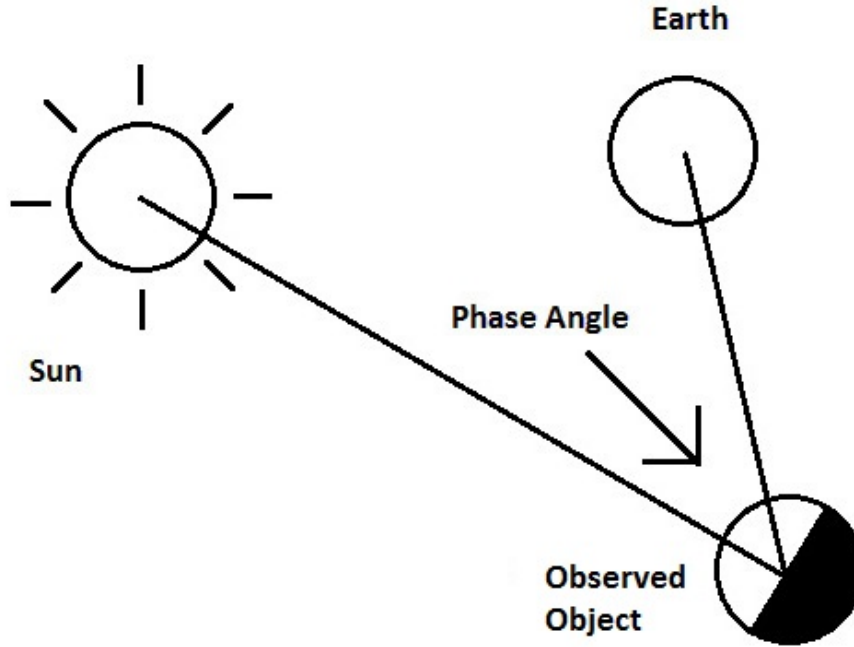


Figure 9: Diagram showing the phase angle schematically.

The absolute magnitude depends only on the properties of the asteroid and is therefore always the same. The apparent magnitude on the other hand also depends on the distance between the asteroid and the observer (in this case the Earth), the distance between the asteroid and the Sun and the phase angle.

It is important to know how to calculate the apparent magnitude, in order to determine if an asteroid can be detected or not. The difference between the absolute and apparent magnitude is caused among others by the varying distance between the object and the Earth and the varying distance between the object and the Sun. Light that comes from an object becomes less intense the further you go away from it. This is because the same amount of light is distributed over a larger area. The area that it will be distributed over a distance D away will be the area of a sphere with a radius D . The area of this sphere is $4\pi D^2$. This means that the area gets x^2 times bigger if the distance to the objects x times bigger. So the brightness gets x^2 times smaller if we are x times further away from the object. If the brightness of an object is 100 times fainter, its magnitude should be 5 smaller. An object that is 100 times fainter is 10 times further away. If we want to convert the absolute magnitude into an apparent magnitude, we have to use how much larger or smaller the distance of the object between the Sun or the Earth is than 1 AU, since that is the distance used in the definition of the absolute magnitude. So if the object is 10 AU away from the Earth or the Sun, the magnitude increases by 5. For any distance from the Earth and Sun, we can say that the magnitude changes by:

$$\Delta_d = 5 \log_{10} \left(\frac{d_{OS} d_{OE}}{(1\text{AU})^2} \right) \quad (1)$$

where d_{OS} is the distance between the object and the Sun and d_{OE} is the distance between the object and the Earth.

3.2 Albedo

Asteroids do not emit light by themselves, their brightness comes from reflected sunlight. Not all light is reflected and scattered away though, some of it gets absorbed. The ratio between the incident Sunlight and the light that is reflected and scattered away is called the albedo. This is always a number between 1 and 0, where 1 means that all light is scattered or reflected away (so the asteroid is a mirror) and 0 means that all light is absorbed (so the asteroid is a black body). The albedo depends on the colour and material of an asteroid. The albedo also depends on the colour, or wavelength, of the incident light. A yellow ball for example has a low albedo for red light, but a high albedo for yellow light. The albedo profile is the albedo as a function of wavelength. A relative albedo profile is shown in figure 10. Asteroids of the same type tend to have albedo profiles with a very similar shape. This is because their composition is similar and composition determines the albedo profile. So if we know the type of the asteroid, its albedo profile can easily be determined. The reason why we want to know the albedo is because an asteroid's absolute magnitude only depends on the rate at which light from the Sun is reflected or scattered, which is the albedo. So

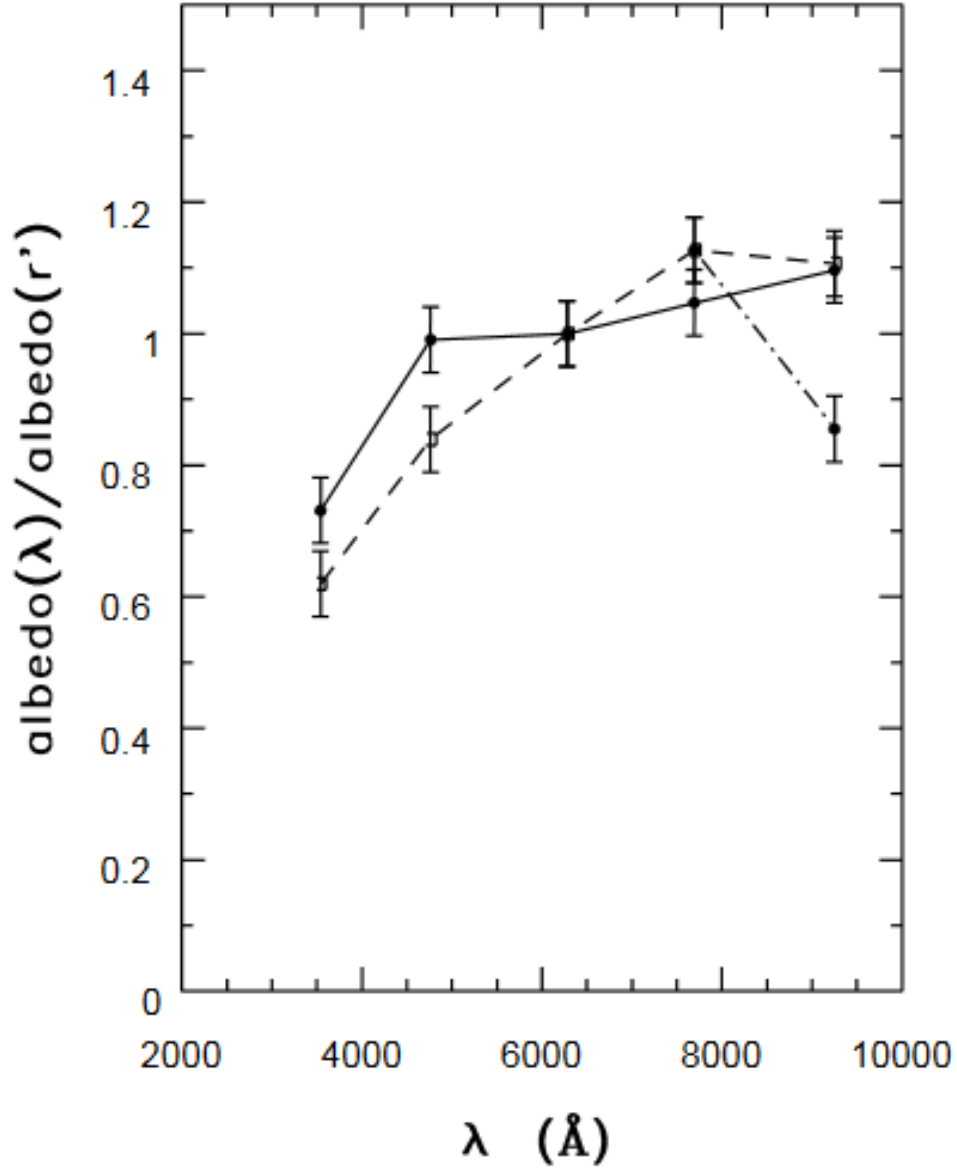


Figure 10: Relative albedo profile with respect to the r^* band for S1-,S2- and C-type asteroids as a function of frequency

if the albedo profile of an asteroid is known, its absolute magnitude can be calculated at every wavelength. We can use formula 2, derived from formula 1 in Harris and D'Abramo

(2015) to determine the albedo of a well known asteroid.

$$p_b = \left(\frac{1329 \text{km}}{D} 10^{-\frac{H_b}{5}} \right)^2, \quad (2)$$

Where p_b is the albedo of the asteroid in a certain band b , D is the diameter of the asteroid and H_b is the absolute magnitude in a certain band b .

3.3 The Slope parameter (G)

The slope parameter is a value invented by the Minor Planet Center, MPC, (MPC) and can be any number, but it is usually between 0 and 1 and almost always 0.15. 0.15 is the standard value for objects for which the slope parameter could not be determined. The slope parameter is related to the shape and geometry of the object. The apparent magnitude (H) is calculated without taking the slope parameter into account, so the slope parameter helps to transform the absolute magnitude into the apparent magnitude. The phase angle and slope parameter can be combined into one component according to Lagerkvist and Williams (1987). In this article, formulae 3, 4, 5, 6 and 7 are derived.

$$\Delta_{G,\alpha} = -2.5 \log((1 - G)\Psi_1(\alpha) + G\Psi_2(\alpha)) \quad (3)$$

$$\Psi_i = W\Psi_{is} + (1 - W)\Psi_{iL} \quad (4)$$

$$W = \exp\left(-90.56 \tan^2\left(\frac{\alpha}{2}\right)\right) \quad (5)$$

$$\Psi_{is} = 1 - \frac{C_i \sin(\alpha)}{0.119 + 1.341 \sin(\alpha) - 0.754 \sin^2(\alpha)} \quad (6)$$

$$\Psi_{iL} = \exp\left(-A_i \left(\tan\left(\frac{\alpha}{2}\right)\right)^{B_i}\right) \quad (7)$$

$\Delta_{G,\alpha}$ is the contribution to the apparent magnitude, due to the phase angle (α) and the slope parameter (G). A_1 , A_2 , B_1 , B_2 , C_1 and C_2 are constants.

So all together, to transform the absolute magnitude into the apparent magnitude formula 8 is used:

$$m = H + \Delta_d + \Delta_{G,\alpha}, \quad (8)$$

where m is the apparent magnitude and H is the absolute magnitude. To actually calculate the apparent magnitude, H , d_{OS} , d_{OE} , α and G are needed.

3.4 The Minor Planet Center

The MPC keeps a list of all known asteroids and comets and some of their properties. These include: semi-major axis, eccentricity, absolute magnitude and many other useful properties. It also lists whether or not an asteroid or comet is a NEO. So that means that we can determine the absolute magnitude of a NEO if we know its name. At the start of

the project this seemed very useful, however as will be clear later on, another method is used to get the absolute magnitude of minor body and comets. Despite this, the MPC is still useful and it will help us in another way. The slope parameter (G) is also listed by the MPC for all minor bodies.

3.5 Trailing loss

There is one more effect we will consider. When telescopes take a picture of the sky, they will integrate for some time. This means that they will look at some point in the sky and gather all photons during that time. It can be compared to a camera with a long exposure time. This is done, because in this way dim objects can also be detected. However this can lead to a problem which actually decreases the added visibility, due to integrating, of an object. If an object moves a significant distance across the sky during the integration time, the light from the object will be smeared out along its travelling direction. The light of a stationary object is spread out over certain pixels in a CCD, so the telescope integrates only those pixels receive all of the light of the object. However if the object starts moving, a larger number of pixels might start receiving light from the object during the integration time. The total light of the object is unchanged, so the object will appear less bright. This effect is called trailing loss. Trailing loss will set in at a certain apparent motion, because the image will not smear if it moves less than a pixel during the integration time. The rate at which trailing loss sets in depends on the resolution and the integration time. The decrease in detectability caused by trailing loss can also be translated to an increase in magnitude. The difference in magnitude between a stationary object and an object with proper motion R is (Harris and D'Abramo, 2015):

$$\Delta_R = 2.5 \log_{10}(R/R_0), \quad (9)$$

where Δ_R is the increase in magnitude due to trailing loss, R is the proper motion of the object and R_0 is the proper motion where trailing loss sets in. Note that the magnitude only increases when R is greater than R_0 . The proper motion is the angle in the sky that the object moves in a certain time.

4 Simulation

The goal of the thesis is to determine if it is possible to detect NEOs using the SASS of BlackGEM. To determine this, we will simulate the observational campaign of the SASS and determine how many NEOs will be detectable by the BlackGEM telescopes. This will be done using a python script which makes use of the SkyBot service (Berthier, Vachier, Thuillot, Fernique, Ochsenbein, Genova, Lainey, and Arlot, 2006). The SASS will be simulated as close to the real survey as possible, however because it is still a simulation, some approximations will be made.

4.1 The Sky Body Tracker project

In order to determine how many NEOs will be seen in a certain field at a certain time, we will use the webservice of the Sky Body Tracker project, SkyBot. SkyBot is an integral part of the algorithm used to simulate the SASS, so it is very useful to understand what it is, how it is used and what it does for us. First of all, SkyBot was made with the intention to provide astronomers with a tool to determine the detections of known Solar System objects in an image. SkyBot has a database containing the pre-computed ephemerides of all known Solar System objects. So SkyBot knows the positions in the sky of all Solar System objects at any point in time. So this means that you can determine what asteroid you are looking at if you know the position in the sky of the asteroid in the picture and the date when the picture was taken. If an astronomer detects an asteroid, comet or other object but does not know the name, they could use SkyBot to identify it. SkyBot has many more uses though, since it also predicts the ephemeris of Solar System objects. It can be used to determine the names of asteroids in a certain field in the sky at a certain time. This will be key to our simulation.

To obtain the list of objects in a certain field at a certain time, an url needs to be visited. The url will look something like this:

```
http://vo.imcce.fr/webservices/skybot/skybotconesearch_query.php?-ep= &-ra= &-dec= &-bd= &-mime= &-output= &-loc= &-filter= &-objFilter= &-refsys= &-from=SkybotDoc
```

This url needs to contain information about the time of the observation, the direction that is pointed in, the location on Earth that was pointed from and the geometry of the field. The date of the measurement can be filled in after ep=, the right ascension should be filled in after ra= and the declination should be filled in after dec=. The right ascension and declination determine the pointing direction of the telescope and the system is comparable to the longitude and latitude system on Earth. The declination is the angle between the vernal equinox, which is a point on the celestial plane, and the projection of the pointing direction on the celestial plane. The right ascension is the angle between the projection of the pointing direction on the celestial plane and the pointing direction on the celestial plane. This is also shown in Fig. 11.

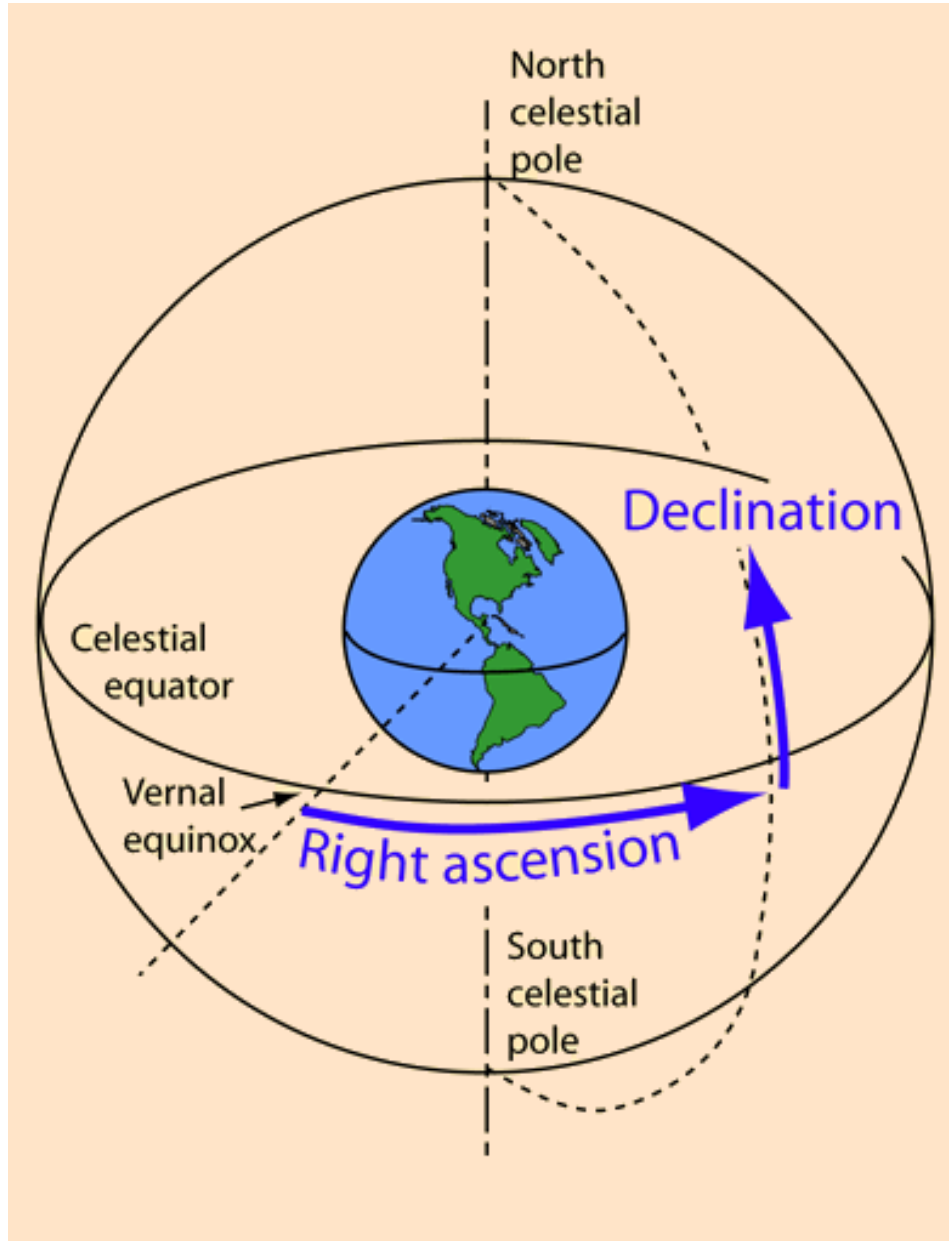


Figure 11: Schematic representation of the right ascension and declination system.

In the url after `bd=`, the dimensions (in degrees) of the field should be filled in, after `loc=`, the location of the observatory should be filled in, the number 809 corresponds to the ESO La Silla location. The other parameters: `mime`, `output`, `filter`, `objFilter` and `refsys` are not dependent on the observation itself, but help with the processing and understanding of the data. `Refsys=EQJ2000&` just means that we use the equatorial right ascension and

declination system as explained above. ObjFilter=100 means that we only want SkyBot to give us the asteroids in the field of interest.

Even though NEOs are defined to be both asteroids and comets, the distinction between asteroids and comets is sometimes hard to make. Near-Earth comets are also far outnumbered by near-Earth asteroids (Harris and D’Abramo, 2015). SkyBot also does not list near-Earth comets explicitly, so it would be impossible to use the information if the comets in view were also requested. I therefore assume that the near-Earth asteroids given by SkyBot include near-Earth comets as well, so that they represent the entire NEO population. If this does not turn out to be true, the result will be close to reality though, because there are very few near-Earth comets. Filter=120 means that we will only consider objects with positional error of less than 120 arcsec. This value is the highest possible, but still ensures that we do not consider objects that have a giant error in their position. Mime=text means that the output is in a text format, which is easiest and fastest to read for code. Output determines the amount of information that is given for each object in the field. Output=obs just means that the information that is given by SkyBot is just enough so that the code can work, but not too much that we are slowed down. With this it is clear how the url for each measurement is made. The parameters: ep, ra and dec will change depending on the observation, while bd, loc, mime, output, filter, objFilter and refsys are the same each time.

There are three different types of results that a SkyBot search can have, these are classified by three different flags: -1, 0 and 1. The first class, flag -1 means that there has been an error, the second class, 0 means that there are no objects in the field at that time and 1 means that there are objects in the field at that time. Examples of these cases are shown in Fig. 12.

An output can be read by the code, so that all asteroids in the field and their properties are known. One of these properties is the object class, which tells us if an object is a NEO or not. If an object turns out to be a NEO we want to determine whether or not it is possible to detect it using BlackGEM. To do that, the apparent magnitude (in the visual band) is obtained from the output of SkyBot. Using these parameters, the apparent magnitude can be computed for every BlackGEM band and so it can be determined if the object is observed.

4.2 Fields of the SASS

Every field is detected 30 times, five times in each of the six BlackGEM bands, during the SASS. To determine how many NEOs are detected over the duration of the entire SASS, we need to determine which fields are visited in which order and at which time which band is measured in. Since we know that each field has the same geometry (a square field with an area of 2.7 square degree) we only need to know the right ascension and declination of the middle of the field to know which field it is. If we can make a list that contains all of the pointing directions, times of detection and bands in which is detected in order, we can request information from SkyBot for all these measurements. The reason why we need

```
# Flag: -1
# Ticket: 163669200463180738
SkyBoT conesearch -> Bad request: epoch cannot be empty or null
```

(a) Example of a flag -1.

```
# Flag: 0
# Ticket: 163804497504058638
No solar system object was found in the requested FOV: RA(deg,hms) DEC(deg,dms):
148.66999999999999 (09:54:40.80) 160.38380000000001 (+160:23:01.68) EPOCH: 2019-07-03
13:43:53.00
```

(b) Example of a flag 0.

```
# Flag: 1
# Ticket: 163660233240660935
# Num | Name | RA(h) | DE(deg) | Class | Mv | Err(arcsec) | d(arcsec)
- | 2008 UG348 | 09 54 35.5207 | +16 26 3.805 | MB>Middle | 23.6 | 0.059 | 197.332
- | 2014 SN240 | 09 54 58.3198 | +16 25 25.788 | MB>Inner | 23.8 | 0.043 | 290.382
216838 | 2006 WD140 | 09 54 35.3589 | +16 27 42.429 | MB>Outer | 21.9 | 0.028 | 291.460
- | 2014 BA70 | 09 54 47.6066 | +16 28 37.443 | MB>Outer | 23.1 | 0.044 | 349.753
- | 2019 BR7 | 09 55 6.3646 | +16 21 40.754 | MB>Middle | 23.2 | 42.830 | 376.714
92362 | 2000 HY29 | 09 54 11.2710 | +16 20 6.557 | MB>Inner | 20.7 | 0.017 | 459.668
- | 2007 DY77 | 09 54 25.6352 | +16 15 59.704 | MB>Middle | 22.8 | 0.329 | 475.100
119863 | 2002 CU123 | 09 55 13.3465 | +16 19 1.194 | MB>Outer | 21.5 | 0.033 | 526.578
- | 2017 SS126 | 09 54 30.5650 | +16 31 41.871 | MB>Middle | 23.2 | 0.104 | 540.627
254535 | 2005 EM139 | 09 55 0.6380 | +16 31 49.266 | MB>Inner | 21.8 | 0.027 | 599.825
439750 | 2015 FC324 | 09 54 11.8954 | +16 15 42.922 | MB>Middle | 21.5 | 0.023 | 604.685
192518 | 1998 RW29 | 09 55 23.0230 | +16 19 1.925 | MB>Middle | 21.2 | 0.026 | 653.317
- | 2005 YF17 | 09 55 24.7246 | +16 27 20.103 | MB>Middle | 22.8 | 0.020 | 682.794
233446 | 2006 HQ106 | 09 54 45.6109 | +16 11 4.018 | MB>Middle | 21.3 | 0.022 | 721.000
- | 2016 GD165 | 09 55 9.8844 | +16 12 28.734 | MB>Inner | 23.4 | 0.050 | 758.925
463428 | 2013 KY16 | 09 54 12.1375 | +16 33 41.882 | MB>Inner | 22.9 | 0.043 | 761.477
77469 | 2001 HZ25 | 09 54 1.8355 | +16 32 28.810 | MB>Middle | 21.6 | 0.024 | 797.377
- | 2017 SB85 | 09 55 12.3035 | +16 33 59.994 | MB>Middle | 23.3 | 0.032 | 799.205
126744 | 2002 CW308 | 09 54 25.5614 | +16 35 59.253 | MB>Outer | 21.4 | 0.028 | 807.877
431008 | 2005 YN78 | 09 55 15.3078 | +16 12 7.065 | MB>Middle | 22.7 | 0.026 | 821.808
20891 | 2000 WN28 | 09 55 7.3812 | +16 35 20.976 | MB>Middle | 19.0 | 0.011 | 832.309
- | 2017 SO125 | 09 55 24.2132 | +16 32 24.530 | MB>Middle | 23.3 | 0.219 | 840.722
```

(c) Example of a flag 1.

Figure 12: Examples of a flag -1 (a), a flag 0 (b) and a flag 1 (c). Flag 1 is an error, flag 0 is no objects in the field and flag 1 is one or more objects in the field.

to request the output from SkyBot in the same field, is because the measurements in the different filters are done slightly after each other. To be precise there is one and a half minute of time between each measurement, this is due to the integration time of one minute and the half of a minute of overhead time. During the integration time, the image is taken and during the overhead time, the filter is changed and the CCD is read out. This small amount of time might not matter in most cases, but sometimes an asteroid moves out of the field in between measurements.

Since the pointing schedule of BlackGEM is not yet finalised, we need to make a pointing schedule to resemble the SASS ourselves if we want to simulate it. A pointing schedule is a list of pointing directions (right ascensions and declinations) and the times at which they are used. I made a list of pointing directions in the Southern sky, such that the fields fill up the entire sky and the fields have no overlap. The fields have a size of 2.7 square degree, or

RA (°)	Dec (°)
0.8215	-89.1785
2.4653	-89.1785
4.1092	-89.1785
...	...
359.1785	-89.1785
0.8215	-87.5114
2.4653	-87.5114
4.1092	-87.5114
...	...
...	...
359.1785	-0.8215

Table 4: Part of list of coordinates of the simulated pointing schedule of the SASS

Field	Time (hh:mm:ss)	Band
Field 1	17:30:00	q
Field 1	17:31:30	u
Field 1	17:33:00	g
Field 1	17:34:30	r
Field 1	17:36:00	i
Field 1	17:37:30	z
Field 1	17:39:00	q
...
Field 1	17:48:00	q
...
Field 1	18:13:30	z
Field 2	18:15:00	q
...
Field 4	20:28:30	z
Field 5	21:00:00	q
...
Field 12	3:28:30	z

Table 5: Part of a schematic overview of the simulated pointing schedule of a simulated night of the SASS.

1.643 by 1.643 degree.

This leaves tiny gaps between the fields in both directions (right ascension and declination), but that also means that the same area will not be surveyed multiple times. In real life this is not a problem of course, since the more information the better but for the simplicity of the code I want to survey the whole sky only once. The gaps between the fields have the size of the skipped sky in a direction over the amount of gaps between the fields that can fit into that direction. So in the case of the right ascension at the equator, there can be 219 fields in that direction, so the size of the skipped sky is: $360 - 219 \cdot 1.643 = 0.183^\circ$ and there are 218 gaps, so the gaps have a size of 3 arcsec. In the case of the declination, there can be 54 fields in that direction and the gaps have a size of 85.2 arcsec. This means that the skipped sky is 1.4 % of the entire Southern sky, because this is such a small amount it can be neglected. The full list of coordinates therefore consists of $218 \cdot 54 = 11772$ fields and part of it is shown in Table 4.

To determine the time of each measurement a starting date needs to be assumed. The starting date that is used in the simulation is the first of December 2018 at 17:00, because that is the start of the night that BlackGEM would have become operational according to early estimates (Bla, a). Since there is no preferred time for NEOs to be in the Southern sky, there is no reason why the starting date should have an influence on the amount of detected NEOs, so it could be an arbitrary date as well. We want to model the SASS as closely as

possible, so we have to make sure that we measure according to the schedule in Fig. 8 and make sure that measurements are only done at night. A night of SASS observations is shown in Table 5. The Table shows how the time passes as other bands and fields are visited. In the simulation it is also taken into account that the SASS is only performed during new Moon, which is not shown in Table 5. Since the SASS measures 30 times in each field through different bands, the asteroids in view need to be determined $30 \cdot 11826 = 353160$, where $11826 = 219 \cdot 54$ is the amount of fields of the SASS. Requesting the SkyBot output takes on average about 12.2 seconds. This maybe looks like a lot, but this is mostly due to the fact that SkyBot is sometimes hard to reach due to connection problems. Simulating the entire SASS causes the code to run for about 50 hours.

4.3 The calculations

Now that we have a method of determining the NEOs that are in the fields during the measurements and some of their properties, we can start to calculate how many NEOs are detected by BlackGEM. To do this, some assumptions need to be made.

4.3.1 Assumptions in the simulation.

The first assumption that needs to be made concerns the type of the asteroids that are present in the fields. The asteroid type determines the albedo profile that the asteroid has, which influences the apparent magnitude in the different BlackGEM bands. Since we don't want to determine whether or not the asteroid gets detected for every possible asteroid type, because the result will become very convoluted very quickly. So we will only consider the most common asteroid types, S-type and the C-type. The relative albedo spectra of these two types are shown in Fig. 10 (Ivezić, Tabachnik, Rafikov, Lupton, Quinn, Hammergren, Eyer, Chu, Armstrong, Fan, Finlator, Geballe, Gunn, Hennessy, Knapp, Leggett, Munn, Pier, Rockosi, Schneider, Strauss, Yanny, Brinkmann, Csabai, Hindsley, Kent, Lamb, Margon, McKay, Smith, Waddell, and York, 2001). In Fig. 10, the solid line corresponds to C-type asteroids and the dotted line corresponds to S-type asteroids. There are 2 different S-type asteroids, we call them S1- and S2-type asteroids. The error bars in the figure are quite large, however for the simplicity of the calculation I assume that the values are absolute and there are no error bars. We want to understand how good BlackGEM is at detecting different types of asteroids. To do this, we assume that every asteroid has the albedo profile of all of the three different types described by Fig. 10. It is then determined whether or not the asteroid is detected for all three cases. Another assumption that is made to simplify calculations is that the BlackGEM bands can be seen as only consisting of the effective wavelength as given by Table 1. This has the effect that the albedo only needs to be evaluated at the effective wavelength. If the whole wavelength band was taken into account, we would have had to integrate the albedo over the entire band. This approach is taken, because the values of the relative albedo do not change much over the bands and because this is an easier and faster way to calculate the albedo for every band and asteroid type combination.

An assumption that has to be made is the assumption that SkyBot’s output is always right and absolute. This means that we do not have to deal with errors. It is also a necessary assumption to make, since SkyBot is the only method we will use to determine the asteroids in the fields.

The proper motion where trailing loss sets in (R_0) is unknown for the BlackGEM telescopes, because this is not needed to achieve BlackGEM’s intended objective. This means that the value for the proper motion where trailing loss sets in needs to be assumed. For most current day surveys, the trailing loss sets in at about 2.5 degrees per day (Harris and D’Abramo, 2015), so this value will be assumed for BlackGEM as well.

4.3.2 Calculating a detection

The apparent magnitude of a NEO needs to be determined in all BlackGEM bands in order to find out if it is detected during a certain measurements. The information we can get from SkyBot is the apparent magnitude in the visible band with an effective wavelength of 5500 Å. This is the only parameter needed to determine the apparent magnitude of the object in each BlackGEM band. The information in Fig. 10 is also used. From Fig. 10, we can read the albedo in each band (BlackGEM or other), relative to the r^* band. The r^* band is introduced in Ivezić et al. (2001) and has an effective wavelength of 6166 Å. This can also be seen from Fig. 10, because that is the wavelength for which all asteroid types have a relative albedo of 1. The relative albedo of the three asteroid types for the BlackGEM bands and visible band is shown in Table 6. V in the band column stands for visible band.

Band	C-type	S1-type	S2-type
u	0.76	0.62	0.62
g	0.99	0.82	0.82
q	1	0.95	0.95
r	1	1	1
i	1.02	1.11	1.11
z	1.1	1.1	0.85
V	1	0.91	0.91

Table 6: Relative albedo in the BlackGEM bands with respect to the r^* band for the three asteroid types.

Formula 2 is used to determine the albedo in the visible band, using the diameter of the asteroid and the absolute magnitude in the visible band. The albedo in the visible band for an assumed asteroid type can be used to determine the albedo in the r^* band, using the relative albedo in Table 6. Using the albedo in the r^* band and the relative albedos in the BlackGEM bands in Table 6, the albedo in the BlackGEM bands can be obtained. This allows us, using the inverse of formula 2, to calculate the absolute magnitude in the BlackGEM bands. We can therefore write an equation that relates the absolute magnitude in the visible band (H_V) to the absolute magnitude in any band. This is shown in equation 10,

$$H_b = 5 \log_{10} \left(\sqrt{\frac{f_V}{f_b}} \right) + H_V, \quad (10)$$

where H_b is the absolute magnitude in the band b , f_V is the relative albedo in the visible band and f_b is the relative albedo in the band b . The diameter dropped out, so formula 10 requires no prior knowledge of the diameter of the asteroid. SkyBot tells us about the apparent visible magnitude of the object though, not the absolute magnitude. This apparent magnitude can be changed into an absolute magnitude, using formulae 1 to 9. This is shown in equation 11:

$$H_V = m_V - \Delta_d - \Delta_{G,\alpha} - \Delta_R. \quad (11)$$

where m_V is the apparent visible magnitude and the other parameters are explained in section 2. Since the distance between the object and the Sun and the Earth, the slope parameter, the phase angle and the rate of motion are needed to calculate this, it looks like this introduces more problems than it solves. However, first of all, these parameters can be obtained from SkyBot which allows us to fill them into equation 11, but second of all, they drop out later on. This happens when we set up equation 12:

$$m_b = H_b + \Delta_d + \Delta_{G,\alpha} + \Delta_R, \quad (12)$$

where m_b is the apparent magnitude in the band b . This equation allows us to turn the absolute magnitude in a band b into an apparent magnitude in the same band b . Together with equation 11, this becomes equation 13:

$$m_b = 5 \log_{10} \left(\sqrt{\frac{f_V}{f_b}} \right) + m_V, \quad (13)$$

where we can see that the only parameters that matter in calculating the apparent magnitude in a band are the relative albedo in the BlackGEM and visible bands. Now that we can calculate the apparent magnitude in any band, we can determine whether or not an asteroid is detected during a measurement. As was stated before and can be seen in Table 5, the SASS measures in one band at a time. So to determine if an asteroid is detected, the code calculates the apparent magnitude in the band corresponding to the time of the measurement. This magnitude is compared to the limiting magnitude in the same band for new Moon, which is when the SASS is preformed, as shown in Table 2. If the limiting magnitude is larger than the apparent magnitude, the NEO is counted as detected and the information of it is stored in a text file. This file also contains the information of the NEOs that were not detected, so they can be compared with each other. A few lines of the file and the header are shown in Fig. 13. The first column of the text file in Fig. 13 shows the time of the measurement in the Julian date, which is the amount of days since January first 4713 BC at 12:00 Universal time. The second and third column show the pointing direction,

```

2459429.279416667 : 165.2054449541284 : 0.0 : g : C : None : None : ['2011 CS4'] : ['414960'] : [0.50782384068187347] : 24.510912013506125 : [24.5]
2459429.279416667 : 165.2054449541284 : 0.0 : g : S1 : None : None : ['2011 CS4'] : ['414960'] : [0.50782384068187347] : 24.613068849843444 : [24.5]
2459429.279416667 : 165.2054449541284 : 0.0 : g : S2 : None : None : ['2011 CS4'] : ['414960'] : [0.50782384068187347] : 24.613068849843444 : [24.5]
2459429.2804383334 : 165.2054449541284 : 0.0 : f : C : None : None : ['2011 CS4'] : ['414960'] : [0.50782199217004731] : 24.338760348080736 : [24.5]
2459429.2804383334 : 165.2054449541284 : 0.0 : f : S1 : None : None : ['2011 CS4'] : ['414960'] : [0.50782199217004731] : 24.338760348080736 : [24.5]
2459429.2804383334 : 165.2054449541284 : 0.0 : f : S2 : None : None : ['2011 CS4'] : ['414960'] : [0.50782199217004731] : 24.338760348080736 : [24.5]
2459429.2811 : 165.2054449541284 : 0.0 : None : None : None : ['2011 CS4'] : ['414960'] : [0.50782384068187347] : 24.42842903383609 : [24.5]
2459429.2811 : 165.2054449541284 : 0.0 : S1 : None : None : ['2011 CS4'] : ['414960'] : [0.50782384068187347] : 24.42842903383609 : [24.5]
2459429.2811 : 165.2054449541284 : 0.0 : S2 : None : None : ['2011 CS4'] : ['414960'] : [0.50782384068187347] : 24.42842903383609 : [24.5]

```

Figure 13: A few lines of the text file containing the result of the simulation.

using the right ascension and declination. The fourth column shows the band in which was detected and the fifth column shows the asteroid type that was assumed for the detection. The sixth and seventh column show the names and ID numbers of the detected NEOs and the eighth and ninth column show the names and ID numbers of all of the NEOs in the field. The tenth column shows the apparent motion of all NEOs in the field, the eleventh column shows the apparent magnitude of all asteroids in the field and the twelfth column shows the apparent V magnitude of all asteroids in the field. These values will be used to draw some conclusions about the properties of asteroids detected by BlackGEM.

5 Results

5.1 interpreting results

After the simulation is completed, another python code will interpret the text file, which will be used to generate results. The text file is read by the code and the contents of the columns are stored into lists. The fields in which no known objects were present can be ignored completely, so their information is removed from the lists. Some objects are detected in all bands and during all measurements in the field, however other objects are only detected in certain bands or move out of the field in between measurements. Whether an object is detected in certain bands or not also depends on the assumed type. If an object is detected at least once in a field and band during the simulation it counts as an object detected by the SASS. Some objects are detected multiple times in different fields, these multiple detections each count as a separate detection.

The names of the objects detected by the SASS are kept in a list, which allows us to count them and determine their properties. When the orbital parameters or other properties of the objects in the fields are needed, the MPC database is used. Because the definition of a NEO is different for SkyBot and the MPC, MPC's list of all minor bodies is used. This still left us with the problem of Kamo'oalewa, but that was quickly solved by linking it to 2016 HO3. The properties of the detected NEOs can be compared to the properties of all NEOs in the fields. This allows us to determine if there is a bias in the detection of NEOs or what fraction of NEOs are detected for example.

5.2 NEOs detection count

The first result that can be shown is the amount of near-Earth objects detected in each band per assumed type, this is shown in Table 7. As stated before, we consider three types of asteroids, C-, S1- and S2-type asteroids. Their albedo profiles are shown in Fig. 10. Objects that are detected in all of the BlackGEM bands are very useful, because in that case the type of the object can be determined. This is because the albedo profile of all asteroid types is known and the albedo profile of an asteroid can be well determined if the asteroid is detected in many different colours. If the albedo profile of an asteroid is known it can be compared to the albedo profiles of the different asteroid types. The asteroid has the type of the albedo profile that corresponds most to its own albedo profile.

5.3 Detection fractions

Although Table 7 is helpful for this particular survey and pointing schedule, the results of the simulation are not representative of the exact BlackGEM detections since the actual pointing schedule will be somewhat different from the one used in the thesis. The detection fraction is a more flexible result. The detection fraction is the amount of detected NEOs over the amount of NEOs that were in the fields over the entire survey. The detection

Band	C-type	S1-type	S2-type
q	1131	1129	1129
u	527	477	477
g	990	962	962
r	766	811	811
i	584	638	638
z	364	379	318
All bands	237	242	203

Table 7: Number of objects detected using the simulated SASS in each band per assumed type. The amount of objects detected in all bands per assumed type is listed in the last row.

fraction can also be a function of absolute magnitude (H) and because H is related to the diameter according to equation 2, a function of diameter. To relate H to the diameter though, an albedo needs to be assumed. A mean albedo of $p_V = 0.14$ is assumed, because it will set an H of 17.5 to a diameter of 1.0 km which is often done in simulations (Harris and D’Abramo, 2015). This value for the albedo is consistent with results from the NEOWISE IR survey (Mainzer, Bauer, Grav, Masiero, Cutri, Dailey, Eisenhardt, McMillan, Wright, and Walker, 2011). The detection fraction is more useful than Table 7, because using a different pointing schedule there may be more or less NEOs in the fields. We can assume that the known NEOs that were in the fields during the simulation, this includes NEOs detected by BlackGEM and NEOs undetected by BlackGEM, are representative all known NEOs, because the SASS surveys the entire Southern sky. Thanks to this, the detection fraction function can be assumed to remain the same for all possible SASS pointing schedules. The detection fraction as a function of diameter is shown in Fig. 14.

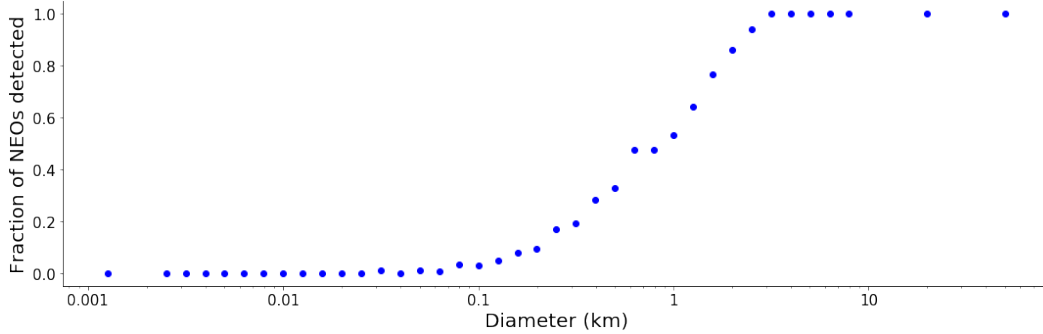


Figure 14: Detection fraction as a function of object diameter using every detected NEO.

Fig. 14 shows the detection fraction for all asteroids in total, however it is also possible to show the detection fraction as a function of diameter in each BlackGEM band and assuming each type. The detection fraction as a function of diameter in each BlackGEM band and assuming each type is shown in Appendix A. It can be seen that the shape of the detection

fraction function for the different types and bands is similar to the function in Fig. 14.

5.4 BlackGEM bias

It could be possible that the NEOs that were detected during the SASS belong to a group that is more easily detected by the BlackGEM telescopes. If this were the case, the orbital parameters of the detected NEOs would be distributed in a substantially different way than the orbital parameters of all the NEOs in the fields. To check if this is the case, histograms of the semi-major axis, inclination, eccentricity and perihelion distance of the detected NEOs and all of the NEOs in the fields are shown in Fig. 15.

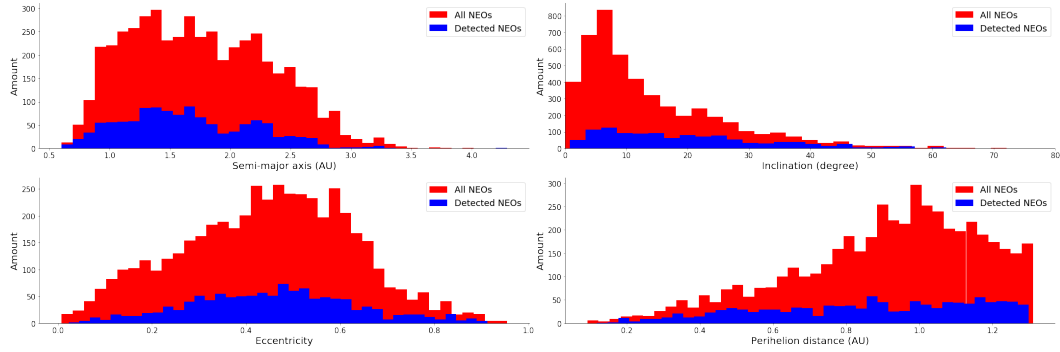


Figure 15: Histograms of the semi-major axis, inclination, eccentricity and perihelion distance of detected NEOs and all NEOs in the fields.

As can be seen in Fig. 15, the distributions of orbital parameters of the detected NEOs have a similar shape to the distributions of all of the NEOs in the fields. This means that the BlackGEM telescopes have no obvious bias towards observing some group of NEOs. Together with the previously made assumption that the known NEOs in the fields of the SASS are representative of the entire known NEO population, we can say that the NEOs detected by the simulated SASS represent the entire known NEO population. This means that the detection fraction of the simulation is the detection fraction of the SASS with any pointing schedule for all NEOs, known or unknown.

5.5 Unknown asteroid detections

An interesting question that arises when the amount of NEOs that can be detected using the BlackGEM telescope array is discussed is how many previously unknown NEOs can be discovered using the SASS. To answer this question, we first need to know how many unknown asteroids there still are. This is of course impossible to know precisely, but the most recent estimations of the unknown NEO size-fraction distribution is shown in Fig. 16. Fig. 16 is based upon data from the MPC and the estimated size-frequency distribution of NEOs (Harris and D'Abramo, 2015). The unknown NEO fraction distribution is the amount

of unknown NEOs with a certain size over the amount of known NEOs with that size for different NEO sizes.

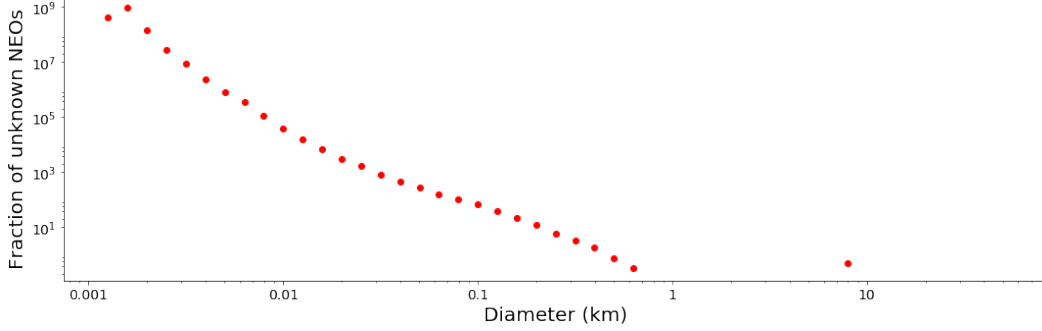


Figure 16: Unknown NEO fraction as a function of NEO diameter, using the MPC database and a NEO size-frequency distribution (Harris and D’Abramo, 2015).

As can be seen from Fig. 14 and Fig. 16 the two fractions are both non-zero around a diameter of 0.2 km. This means that the BlackGEM telescopes can detect NEOs in a diameter range where there is still a reasonable fraction of unknown NEOs. We already assumed that the detection fraction is the detection fraction for the total known NEO population. If we assume that the total known NEO population is representative of the total NEO population, the detection fraction can be defined as in equation 14:

$$f_{Det} = \frac{D_{tot}}{I_{tot}} = \frac{D_k + D_u}{I_k + I_u}, \quad (14)$$

where f_{Det} is the detection fraction, D_{tot} is the total amount of NEOs detected by the SASS, this consists of the known NEOs (D_k) and the unknown NEOs (D_u). I_{tot} is the total amount of NEOs in the fields, this consists of the known NEOs (I_k) and the unknown NEOs (I_u). From the simulation we know f_{Det} , D_k and I_k . Because we assumed that the distribution of the NEOs in the fields of the simulation is representative for the entire NEO population, the unknown NEO fraction can be defined as in equation 15:

$$f_u = \frac{N_u}{N_k} = \frac{I_u}{I_k}, \quad (15)$$

where f_u is the unknown NEO fraction, N_u is the total amount of unknown NEOs, N_k is the total amount of known NEOs, I_u is the total amount of unknown NEOs in the fields and I_k is the total amount of known NEOs in the fields. Equation 14 and 15 can be combined to yield equation 16:

$$D_u = f_{Det} (f_u + 1) I_k - D_k, \quad (16)$$

where all of the parameters are functions of diameter and all except for D_u are known. If all of the knowns are filled in, the amount of previously unknown NEOs that can be

detected using the SASS as a function of their diameter can be determined. This is shown in Fig. 17.

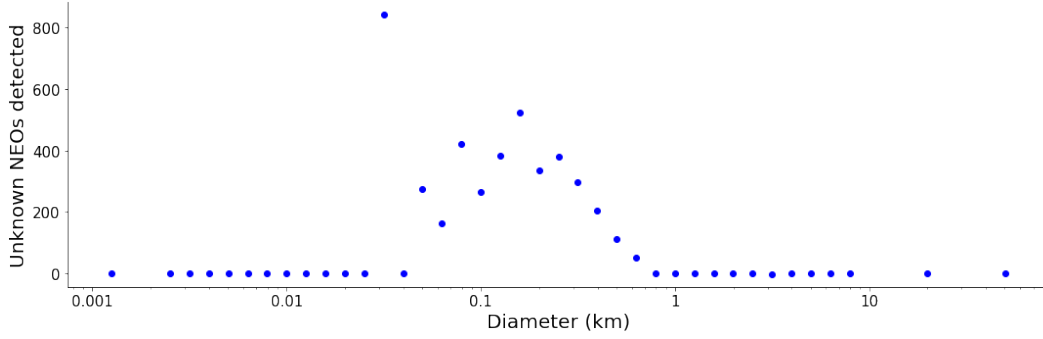


Figure 17: Predicted amount of currently unknown NEOs detected using the SASS as a function of diameter.

In Fig. 17, it can be seen that most of the new detections will have a diameter around 0.2 km. PHOs have a diameter of at least 140 m, so it can be possible that the BlackGEM telescope array can help to detect new Potentially Hazardous Objects. The predicted total amount of previously unknown NEOs detected during the SASS is equal to the sum of the previously unknown NEOs detected with each diameter in Fig. 16. This is equal to 4244 previously unknown NEOs, so the real SASS should discover around 4000 previously unknown NEOs.

6 Discussion

6.1 Assumptions

There are some assumptions made during the research. Some of these assumptions might introduce certain limitations, so they should be discussed.

The first of these assumptions is that the total known NEO population is representative of the total NEO population. This might not be entirely true though. The known NEOs have been discovered during previously preformed minor body surveys. Brighter NEOs or NEOs that come closer to the Earth more often due to their orbit get detected more easily. Minor body surveys generally detect more often in the ecliptic plane, because that is where most of the minor bodies orbit. However there still are minor bodies with a high inclination, which means that generally their detection fraction is lower than minor bodies with a lower inclination. Because the minor bodies that are easier to detect are already detected, detecting the remaining unknown objects should be harder than redetecting known objects. However this does not hold for minor bodies with a large inclination, because the SASS detects in the entire Southern sky, it has an easier time detecting minor bodies with a large inclination. So the estimated amount of predicted discoveries of NEOs is probably too large, except for NEOs with a high inclination, for which it is probably too small.

Another assumption is that objects brighter than the limiting magnitude are detected and objects fainter than the limiting magnitude are not detected. This assumption was used to simplify the simulation code. In reality, the limiting magnitude is the magnitude for which the S/N is equal to 5. This means that the chance that the object is detected is almost 100 %. This is similar to the assumption that any object brighter than the limiting magnitude is detected. However, as the apparent magnitude of the object becomes larger than the limiting magnitude, it does not mean that the object is not detected, the probability that it is detected just becomes smaller. So the amount of NEO detections would in reality most likely be bigger than in the simulation, due to this effect.

Another, sometimes implicit, assumption is that the information used by the simulation is always correct and without uncertainty. This is of course not true, but it makes the simulation possible. One of the places where this assumption might break down is at the values of the relative albedo. In Fig. 10 there are clearly error bars in the value of the relative albedo, but during the simulation these are ignored. This causes the result of the simulation to be a bit less reliable, there could be more or less detections, depending on the type. Another place where the assumption might break down is by assuming that the information from SkyBot is perfect. For many known NEOs and asteroids in general, the orbital parameters are not known precisely enough to determine the orbits without error. In the code, no errors in the position are taken into account, this means that objects that were simulated to be in the fields during the SASS might have been outside of it in reality. But objects that were simulated to be outside the fields could also have been inside of it. So even though this effect might have an influence on the outcome of the simulation, we can not say if the real result would mean more or less detections.

6.2 Code improvements

A part of the code that can still be improved on is definitely the speed. As stated before, it takes 50 hours to fully simulate the SASS. The slowest part of the code is the part that loads the SkyBot output. It takes between 0.1 seconds and sometimes even 10 minutes (due to high traffic most likely) to load the output, while all the other parts of the code together take negligible time. Currently the speed of the code has not been improved, but there are some simple things that can be done to speed up the code. First of all, different parts of the simulation can be run in different kernels at the same time. The first few divisions would reduce the time it takes by a lot and it is very simple to divide the fields up among the different kernels. The disadvantage of this method is that it is quite hardware expensive to use multiple kernels for this end. It could also be possible that the code could be improved such that multiple fields are evaluated at the same time, however this goes beyond the scope of the thesis but can be improved at a later time.

Another part of the code that can still be improved is the way that the pointing scheme in table 4 is created. The problem with the pointing scheme is that in trying to limit the amount of overlap between the fields, a lot of overlap was created at the South pole. This is because naively, the separation between the fields remains constant at every declination. At a near-zero declination, this is not a problem and the fields have some space between them. However at higher declinations, the space between the fields becomes smaller and eventually they will overlap. This is because the amount of sky that is covered by a square degree becomes smaller when the declination becomes higher. The amount of sky covered by a field stays the same, so if the same amount of fields are kept in a certain declination, they will eventually overlap. This overlap is largest at the poles, however this is also the place where the least amount of NEOs are present. So the chance that any NEOs got observed many more times than they would without overlap is small. However by decreasing the amount of fields per declination at higher declinations, the speed of the simulation would increase. So it is definitely worthwhile to improve the tiling scheme of the simulation for future use.

There are still some other parts of the code that are unoptimized. For instance the function that calculates the apparent magnitude for the different bands still relies on an input diameter, distance between the NEO and the Sun and the Earth, phase angle and slope parameter. Since it is clear from equation 13 that those parameters are not necessary, the code can be improved by removing its dependence on those. There are other similarly small parts in the code that make it more convoluted than it should be, however, improving them would neither speed up the code nor yield better results. The only thing that would improve is the way it looks, so that it is easier to read and understand. Despite that it is still definitely worth it to do.

6.3 Further research

There is still some possible further research that can be done. For instance, we only considered detecting NEOs with the SASS, however it might also be possible to use any of the

other BlackGEM surveys to detect NEOs. This possibility can be researched by simulating the other surveys, much like we did with the SASS.

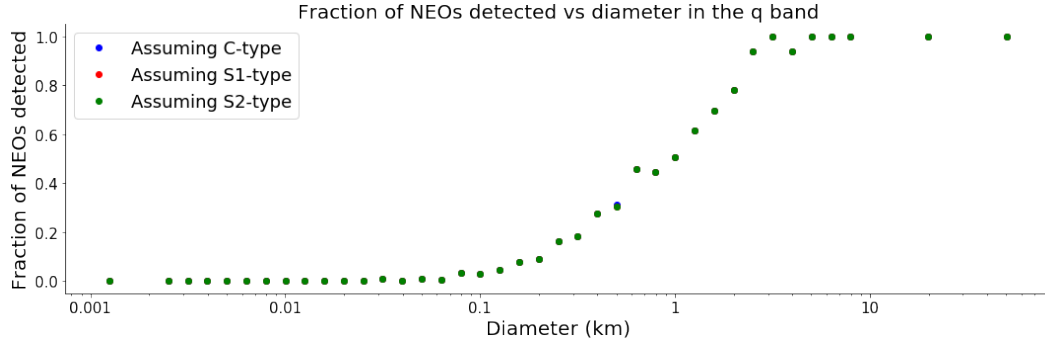
The simulation was done using the known NEO population with SkyBot. However, a different minor body population could also be used to simulate the SASS with. This population could for example be a prediction of the NEO size-frequency distribution, or something else entirely. In that case SkyBot can not be used, but the result might give more insight in the detection of previously unknown NEOs or give a more accurate (re)detection fraction.

While writing the code for the simulation it became clear that there is a difference between the definition of NEO by the MPC and SkyBot. It could be interesting to investigate this further to see what caused this difference.

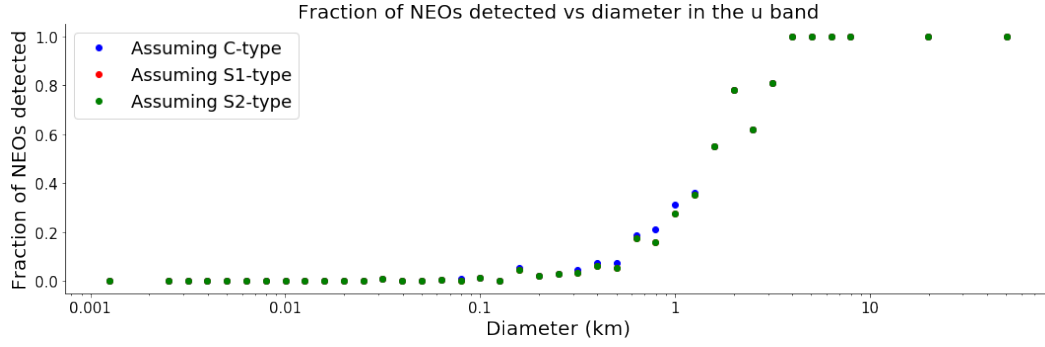
7 Conclusion

Using a simulation of the SASS we have shown that it is possible to (re)detect known NEOs with the BlackGEM telescopes. Furthermore it is determined that the SASS has no bias in observing NEOs, so NEOs observed by the SASS are accurate representation of the total NEO population. This allowed us to determine that the predicted amount of detected previously unknown NEOs is 4244. Most of these newly discovered NEOs have a diameter around 200 m. This is an interesting size, because there are still unknown potentially hazardous objects around those sizes. Discovering potentially hazardous objects is extremely useful, because it might warn us early if they were on collision course with the Earth. Since the pointing schedule of the real SASS will most likely not be the same as the pointing schedule of the simulate SASS, the exact amount of (re)detections and previously unknown discoveries will most likely not be the same for the real SASS. However, because the real SASS will survey the same population in the same part of the sky, it is likely that the amount of detections done by the real survey is similar to the amount of detections done by the simulated survey. We can therefore conclude that the BlackGEM telescope array can be used to (re)detect known NEOs and discover currently unknown NEOs.

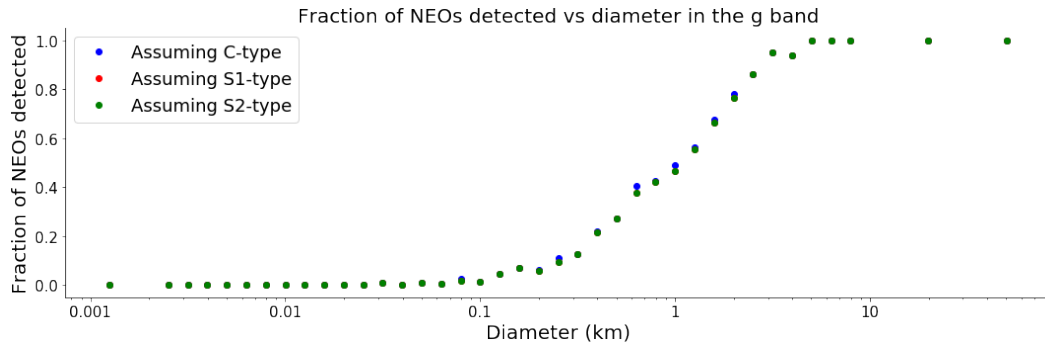
8 Appendix A: detection fractions as a function of diameter in each BlackGEM band



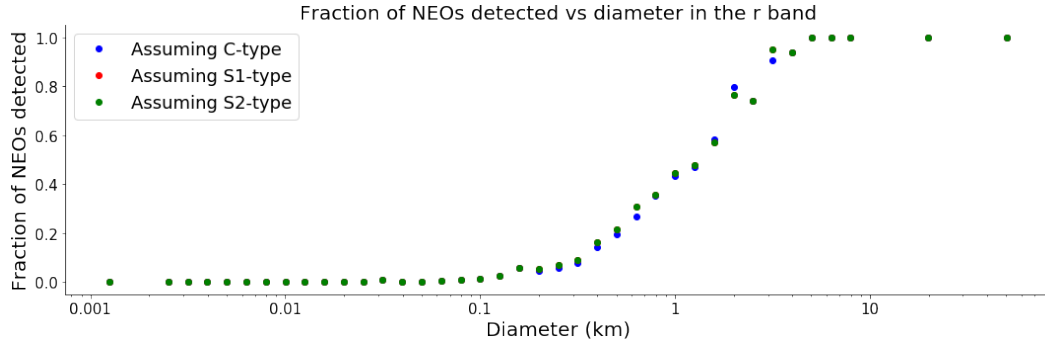
(a)



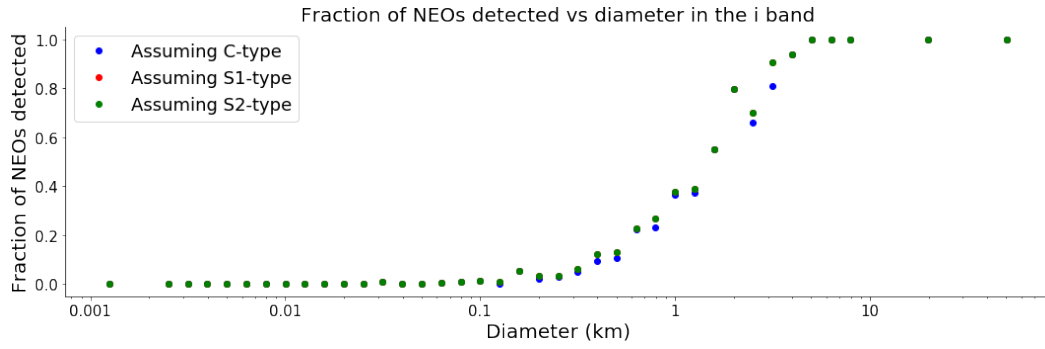
(b)



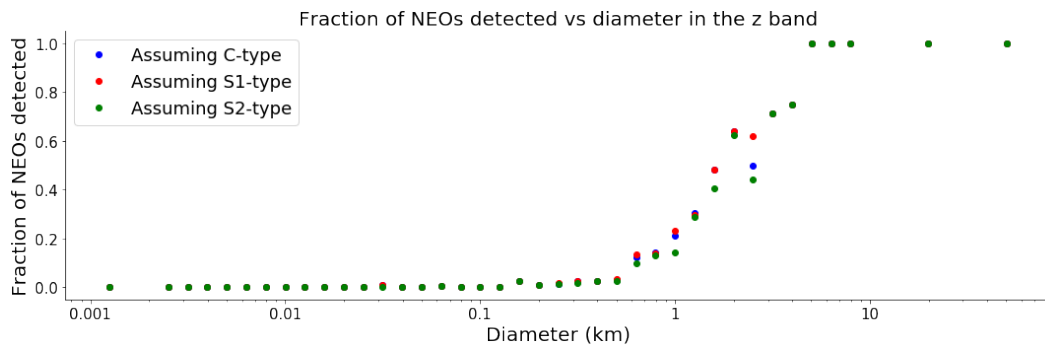
(c)



(d)



(e)



(f)

Figure 18: Detection fraction as a function of diameter for every band assuming every type.

9 Appendix B: Problems, solutions and possible improvements

During the coding of the simulation, some problems came up that needed to be solved. One of the more interesting problems came up when the MPC was used to determine properties of the NEOs in the field. This was done by searching for the names of the NEOs in the field in the MPC's NEO list and reading the properties from the row that corresponds to these names. However it turned out that sometimes the name of SkyBot's NEO could not be found in the MPC's NEO list. After some searching, it was found out that these objects were in MPC's list of all minor Solar System objects. This means that some objects that are classified by SkyBot as NEOs are not actually NEOs according to the MPC. This problem was solved easily by using MPC's list of all minor Solar System objects instead of the list with only NEOs. However there was still one exception. The asteroid Kamo'oalewa was previously known as 2016 HO3, SkyBot however still uses 2016 HO3 as its name, while MPC uses Kamo'oalewa. The code could therefore not correspond these two with each other, however after learning that the name 2016 HO3 changed into Kamo'oalewa the problem was quickly solved. Many asteroids have an ID number together with their name, Kamo'oalewa's ID is 469219. This ID number always stays the same but not all asteroids have one, so searching for only the ID in the MPC list was not an option. As a second option though it is enough to use the ID as a way to determine the properties of the NEOs in the fields. It is still interesting and good to know though that there is a difference in the definition of a NEO according to SkyBot and the MPC.

Another problem that came up when the full simulation was done was that, when the internet connection was unstable, the connection to SkyBot would fail and the code would give an error and stop. This was be very annoying when the code was going to run for the entire night, only to stop after a few minutes when the connection was interrupted. However, this problem can be solved by looping infinitely over the entire part of the code that determines a detection and passing any exception that occurs. Passing an exception means that when the code gives an error, it will skip the part in which the error occurred and continue running. If we loop over that it means that we start over any time an error occurs. This ensures that the code will keep on running, even when the connection to SkyBot is lost. However this gave rise to another problem, it was now very difficult to stop the code from running, since any error would just cause the code to start over again. An exception was therefore put in place that a keyboard interruption, which is an interruption that is done by hand, would actually cause the code to stop. Then there was one final problem left, the code would continue to run, even when the SASS was completely simulated. This is unwanted, because it would drain computer power unnecessarily. This was solved by not letting the loop go indefinitely, but until the SASS was completely simulated. These solutions were vital to allow the code to run smoothly for 50 hours.

10 Appendix C: SASS simulation code

```
#Just some imports

#Numpy is used to work with better lists
import numpy as np
#Urllib.request is used to acces the SkyBot database
import urllib.request
#import math
#import os
#import astropy
#Time is used to find out how long some parts of the code take
import time
from matplotlib.pyplot import figure, show
import matplotlib.pyplot as plt
#Just making it easier to use pi
pi = np.pi

#Downloading the file from the MPC that contains information about all known
#asteroids

url = 'https://www.minorplanetcenter.net/iau/MPCORB/MPCORB.DAT'
urllib.request.urlretrieve(url, 'asteroidfile.txt')

#Below is the code that helps to make the different urls to acces the SkyBot
database

#Make the list that gives the order in which the different bands are adressed every
#field
bandorder = np.tile(['q','u','g','r','i','z'],5)
#Amount of bands that is measured in per field
nb = len(bandorder)
#Number of fields in the right ascension, if there is no overlap
#Nfields = (360/1.643)
#List of different fractions of the number above, used to compare differently sized
#parts of the sky with eachother the
#final entry must always be 1, since it should be the full list
Nfieldslist = Nfields*np.array([1/40,1/25,1]) #,1/10,1/5,1/3)
#Apparent magnitude limit of Blackgem for the different bands at new moon, which is
#good for the SASS
magmax = [22.7,21.3,22.4,21.7,21.2,20.3]
#Lists of lists of Epochs, Right ascensions and declinations, used to make the urls
#to acces SkyBot
```

```

BotEpochlist = []
RAlist = []
Declist = []
#A list of Epoch, RA, and Dec will be made for every entry of Nfieldslist, these
#lists will be stored in the lists above
for i in np.arange(len(Nfieldslist)):
    #The length of the lists below is equal to the amount of fields in the right
    ascension times the amount of fields in
    #the declination times nb, because it is the total amount of fields investigated
    #times the amount of filters per field
    #The entry in Nfieldslist
    Nfields = Nfieldslist[i]
    #Time gap between measurements, due to the Local transient survey that happens
    #after every 4 fields and lasts 1/2 hour
    LTStime = ((np.arange(nb*int(Nfields)*int(Nfields/4))/(4*nb)).astype(int))/48
    #Time gap between measurements due to the fact that there are no measurements
    #done during the day, happens after 12
    #fields and lasts 13.5 hours
    Daytime = ((np.arange(nb*int(Nfields)*int(Nfields/4))/(12*nb)).astype(int))*
    13.5/24
    #Epoch, the list that tells at which time a filter is used, a filter has an
    #integration time of 1 min and a switch
    #time of 30 sec.
    BotEpochnrlist = 2458454.02525 + 1.5/24/60 * np.arange(nb*int(Nfields)*
    int(Nfields/4)) + LTStime + Daytime
    #We need strings to make the url
    BotEpoch = BotEpochnrlist.astype(str)
    BotEpochlist.append(BotEpoch)
    #Right ascensions (degree), this list goes from the middle of the FOV to 360
    #minus the middle of the FOV and contains
    #int(Nfields) entries
    RAss = np.linspace(1.643/2,360-1.643/2,int(Nfields))
    #Since we look at the same field nb times in a row, we use np.repeat to repeat
    #every entry nb times in a row
    RAs = np.repeat(RAss,nb)
    #Since we go through the right ascensions for every declination, the above list
    #needs to be followed by itself for
    #every declination. There are half as many declinations as right ascensions.
    RA = np.tile(RAs,int(Nfields/4))
    RAlist.append(RA)
    #Declination (degree), this list goes from -90 plus the middle of the FOV to 90
    #minus the middle of the FOV and
    #contains int(Nfields/4) entries
    Decss = np.linspace(-90+1.643/2,0,int(Nfields/4))

```

```

#Since we look at the same field nb times in a row, we use np.repeat to repeat
#every entry nb times in a row
Decs = np.repeat(Decss,nb)
#Since we go to the next declinations for every full set of right ascensions,
#the entries of the above list need to be
#int(Nfields) times in a row.
Dec = np.repeat(Decs,int(Nfields))
Declist.append(Dec)

#Prints are used to debug
#print(len(BotEpochlist[0]),len(RAlist[0]),len(Declist[0]),nb*int(Nfields)*
int(Nfields/4))
#print(BotEpochlist[0])
#print(float(BotEpochlist[0][-1])-2458454.02525)

#The size of the field in degrees, its a 1.643 by 1.643 square
bd = "1.643x1.643"
#How we want the data exported, always text
mime = "text"
#How much data we get, can be changed, obs should be enough
output = "obs"
#809 is the code of the location: ESO La Silla (https://minorplanetcenter.net/iau/lists/ObsCodes.html)
observer = 809
#Only asteroids with a position error less than this in arcsec are shown, should be
#the same for all observations,
#but not sure yet what
filt = 120
#What objects we're looking for, 100 is only asteroids
obj = "100"
#Reference frame for coordinates, should look up but probably EQJ2000
refsys = "EQJ2000"

#Print is used to check some stuff
#print(max([len(str(Declist[-1][i])) for i in np.arange(len(Declist[-1]))]) )

#Function to split up the text file according to the sizes found at:
#https://www.minorplanetcenter.net/iau/info/MPOrbitFormat.html
def slices(s, x):
    position = 0
    result = []
    for length in x:
        if length > 0:
            #Most entries of the text file are not as long as the sizes found above,

```



```

        #so the strings contain a lot of
        #spaces in front and behind the keyword we want to save. The .join bit
        #is to remove exces spaces but keep
        #spaces in between, so that names with spaces stay intact
        result.append("└".join(s[position:position + length].split()))
        position += length
    #causes negative values in x to skip that many spots.
    elif length < 0:
        position += abs(length)
    return result

#Below is the code that determines the detection rules

#Rate of motion when trailing loss sets in in deg/day
R0 = 2.5
#The different bands (I put V in for calibration if pr != pV)
bandnames = ['q','u','g','r','i','z','V']
#The types of asteroids we use
Typelist = ['C','S1','S2']
#Relative Albedo for the different bands for C-type (relative to pr ~ pV)
CrelPlist = np.array([1,0.76,0.99,1,1.02,1.1,1])
#Relative Albedo for the different bands in the order of the bandnames list for
S1-type (relative to pr ~ pV/0.91))
S1relPlist = np.array([0.95,0.62,0.82,1,1.11,1.1,0.91])
#Relative Albedo for the different bands in the order of the bandnames list for
S2-type (relative to pr ~ pV/0.91))
S2relPlist = np.array([0.95,0.62,0.82,1,1.11,0.85,0.91])
#"Typical" diameter in m (doesn't matter though, because we already have apparent V
magnitude from SkyBot)
D = 1200

#Alpha is in degrees, formula gotten from Lagerkvist 1987
def q(G,A1,A2,B1,B2,C1,C2,alpha):
    #The calculations below should be clear from the article, since the same
    #variable names are used
    W = np.exp(-90.56*(np.tan(alpha*pi/360))**2)
    psi1s = 1-(C1*np.sin(alpha*pi/180))/(0.119+1.341*np.sin(alpha*pi/180)-0.754
    *(np.sin(alpha*pi/180))**2)
    psi2s = 1-(C2*np.sin(alpha*pi/180))/(0.119+1.341*np.sin(alpha*pi/180)-0.754
    *(np.sin(alpha*pi/180))**2)
    psi1L = np.exp(-1*A1*(np.tan(alpha*pi/360))**B1)
    psi2L = np.exp(-1*A2*(np.tan(alpha*pi/360))**B2)
    psi1 = W*psi1s + (1-W)*psi1L
    psi2 = W*psi2s + (1-W)*psi2L

```

```

    return (1-G)*psi1+G*psi2

#Formula for the absolute magnitude in different bands using the albedo and diameter
#, via the apparent visual magnitude,
#using Harris 2015
def Hcalc(D, relp, Vapp, dBS, dBO, G, A1, A2, B1, B2, C1, C2, alpha):
    #Changes the apparent V magnitude to an absolute V magnitude using the
    #semi-empirical HG system
    Vabs = Vapp + 2.5*np.log10(q(G, A1, A2, B1, B2, C1, C2, alpha))-5*np.log10(dBS*dBO)
    #Calculates the visual albedo using the formula in Harris 2015
    pV = (1329000/D*10**(-1*Vabs/5))**2
    #Calibrates the relative albedos to get the albedo in all bands
    P = relp*pV/relp[-1]
    #Returns a list of the absolute magnitude (H) in the different bands
    return 5*np.log10(1329000/(D*np.sqrt(P)))

#Semi-empirical HG system for apparent magnitude, used by the MPC
#dBS and dBO are in AU
def vismag(D, relp, Vapp, dBS, dBO, G, A1, A2, B1, B2, C1, C2, alpha):
    return Hcalc(D, relp, Vapp, dBS, dBO, G, A1, A2, B1, B2, C1, C2, alpha)+5*np.log10(dBS*dBO)
    -2.5*np.log10(q(G, A1, A2, B1, B2, C1, C2, alpha))

#constants for q from Lagerkvist 1987
A1 = 3.332
A2 = 1.862
B1 = 0.631
B2 = 1.218
C1 = 0.986
C2 = 0.238

#Below is the code used to extract data from the MPC site

#The file I saved in the second code block, from the MPC site
file = open('asteroidfile.txt', 'r')
#the width of the columns found at: https://www.minorplanetcenter.net/iau/info
#/MPOrbitFormat.html
fieldwidths = [7,-1,5,-1,5,-1,5,-1,9,-2,9,-2,9,-2,9,-2,9,-1,11,-1,11,-2,1,-1,9,-1,
5,-1,3,-1,9,-1,4,-1,3,-1,3,-1,10,-1,4,-1,8,-1,19,8]

#loop that is used to create columns from the MPC file, using the fieldwidths given
#above. This method is used, because
#some colums are missing or empty and the splices function, introduced in block 4,

```

```

#can deal with that
Alllist = []
row = 0
startrow = 0 #43 #0
for line in file:
    if row >= startrow:
        fields = line.split(";")[0]
        Alllist.append(slices(fields,fieldwidths))

    row +=1

#The stuff below creates lists with asteroid properties from Alllist
n = len(Alllist)
#just to see how many asteroids we know of
print(n)
#Number of the asteroid
Nr = []
#Absolute H magnitude of the asteroid, some asteroids may not have value
H = []
#Slope parameter of the asteroid, some asteroids may not have value
G = []
#Epoch of the asteroid
Epoch = []
#Mean anomaly at epoch (deg)
MaEpoch = []
#Argument of perhelion (deg)
ArgofPer = []
#Longitude of ascending node (deg)
LongAN = []
#Inclination of ecliptic (deg)
Inc = []
#Eccentricity
e = []
#Mean daily motion (deg/day)
MDM = []
#semi-major axis
a = []
#Uncertainty parameter, U some asteroids may not have value
U = []
#Reference
Ref = []
#Number of observations
NrObs = []
#Number of oppositions

```

```

NrOpp = []
#Year of first and last observation, or Arclength
Var = []
#R.m.s. residual (arcsec)
RMSres = []
#Course indication of perturbers
CPert = []
#Precise indication of perturbers
PPert = []
#Computer name
PC = []
#4-hexdigit flags
flag = []
#ID of the asteroid, some asteroids may not have value
ID = []
#Name of the asteroid, used to relate the MPC file to the SkyBot result
Name = []
#Date of last observation
Date = []

for i in np.arange(n):
    Nr.append( Alllist[i][0])
    H.append( Alllist[i][1])
    G.append( Alllist[i][2])
    Epoch.append( Alllist[i][3])
    MaEpoch.append( Alllist[i][4])
    ArgofPer.append( Alllist[i][5])
    LongAN.append( Alllist[i][6])
    Inc.append( Alllist[i][7])
    e.append( Alllist[i][8])
    MDM.append( Alllist[i][9])
    a.append( Alllist[i][10])
    U.append( Alllist[i][11])
    Ref.append( Alllist[i][12])
    NrObs.append( Alllist[i][13])
    NrOpp.append( Alllist[i][14])
    Var.append( Alllist[i][15])
    RMSres.append( Alllist[i][16])
    CPert.append( Alllist[i][17])
    PPert.append( Alllist[i][18])
    PC.append( Alllist[i][19])
    flag.append( Alllist[i][20])
    ID.append( Alllist[i][21])
    Name.append( Alllist[i][22])

```

```

Date.append( Alllist [ i ][ 23 ])

floata = np.array ([ float (ah) for ah in a if ah != '' ])
floate = np.array ([ float (eh) for eh in e if eh != '' ])
floati = np.array ([ float (ih) for ih in Inc if ih != '' ])

q = floata*(1-floate)
Q = floata*(1+floate)

Amors = 0
Appollos = 0
Atens = 0
Atiras = 0
for num,ah in enumerate(floata):
    if ah > 1:
        if q[num] > 1.017:
            Amors +=1
        else:
            Appollos += 1
    else:
        if Q[num] > 0.983:
            Atens += 1
        else:
            Atiras += 1

print(Amors, Appollos, Atens, Atiras)

fig = figure(figsize=(30, 8))
fr = fig.add_subplot(1,2,1)
fr.scatter(floata ,floate , c = 'black', marker = 'o', alpha = 1, s = 1)

fr.spines[ 'right' ].set_visible(False)
fr.spines[ 'top' ].set_visible(False)

fr.set_ylabel("Eccentricity",fontsize = 20)
fr.set_xlabel("Semi-major_axis_(AU)",fontsize =20)
fr.set_xlim(0,6)
fig.tight_layout()
fr.tick_params(axis='both', which='major', labelsize=14)

fr = fig.add_subplot(1,2,2)
fr.scatter(floata ,floati , c = 'black', marker = 'o', alpha = 1, s = 1)

fr.spines[ 'right' ].set_visible(False)

```

```

fr.spines[ 'top' ]. set_visible( False)

fr.set_ylabel("Inclination_(degree)", fontsize = 20)
fr.set_xlabel("Semi-major_axis_(AU)", fontsize =20)
fr.set_xlim(0,6)
fr.set_ylim(0,80)
fig.tight_layout()
fr.tick_params(axis='both', which='major', labelsize=14)
show()

#The code below is the final code that goes through the full list of coordinates
#and saves the result in a file that can
#also be read to see how far we are

#While loop so that the code always keeps running
loop = True
while loop == True:
    #Try to run the code until an error occurs (most often connection error)
    try:
        #Making a file that stores the results from the code below. If it already
        #exists it will not create a new one.
        try:
            file = open("BachResultfinal.txt", 'x')
            header = "#Epoch;_RA;_Dec;_band;_type;_Detected_Name(s);_Number(s)"
            "of_detected;_In_view_Name(s);_Number(s)_of_in_view;_Apparent_motion"
            "of_NEO(s)_in_view;_Apparent_magnitudes_of_NEO(s)_in_view;_Apparent_V"
            "magnitude_of_NEO(s)_in_view\n"
            file.write(header)
            file.close()
        except:
            pass

        #Since the file always contains the header, the amount of measurements we
        #have already done is the amount of lines
        #minus 1divided by x, since every measurement gives x lines, where x is
        dependent on the amount of types we assume
        #and wether or not we look at the impact of trailing loss
        linespmeas = len(Typelist)
        nstart= (sum(1 for line in open('BachResultfinal.txt')) - 1)/linespmeas

        #If the code stopped while it was writing results in a certain field
        (very rare) nfields will not be integer, in that case
        #I will remove the inputs of the final field and repeat the measurement of
        that field

```

```

if nstart - int(nstart) > 0:
    print("Code_was_interrupted_during_result_writing")
    with open("BachResultfinal.txt", "r") as f:
        lines = f.readlines()
    with open("BachResultfinal.txt", "w") as f:
        for inde, line in enumerate(lines):
            if len(lines)-inde - 1 >= nstart%len(Typelist) :
                f.write(line)

#Setting nstart to an integer, so that the rest of the code understands
#it and so that if it wasn't it would go
#down to the first integer below, which is what we want after removing
#some entries from the file
nstart = int(nstart)

#List of Epochs/RAs/Decs corresponding to the Nfield with index -1, because
#They start where the file has ended
BotEpoch = BotEpochlist[-1][nstart::]
RA = RAlist[-1][nstart::]
Dec = Declist[-1][nstart::]
#Used to keep track of how long the code is going to take while it is
#running
N = len(BotEpoch)

#After how many fields we should tell how far to go and how long it took
interval = 1000

#Timer to show how long each interval took
jstart = time.time()

#Tell how far wer are at the start and how much we still need to do
print("At_the_start_we_had_already_done_{ }_fields".format(nstart))
print("")
print("We_still_have_{ }_fields_to_go.".format(N))

#Go through all fields
for j in np.arange(N):
    #Used to see how far we are (used for debugging)
    #print(j)
    #Url of SkyBot we want to visit
    urlopen_in = "http://vo.imcce.fr/webservices/skybot/skybotconesearch_"
    "query.php?-ep="+BotEpoch[j]+'&-ra='+str(RA[j])+'&-dec='+str(Dec[j])+"
    "&-bd="+bd+'&-mime='+mime+'&-output='+output+'&-loc='+str(observer)+"
    "&-filter="+str(filt)+'&-objFilter='+str(obj)+'&-refsys='+refsys+'&-"
```

```

"from=SkybotDoc"
#Print used to debug
#print(urlopen_in)
u=urllib.request.urlopen(urlopen_in)

#Making the loaded code into something useable
result=urllib.urlopen(urlopen_in).read()
u.close()

#The stuff below is only possible when mime is text and is basically
#making the result list readable
splitted1 = np.array(result.split('\n'))
n1 = splitted1.size
splitted2 = np.delete(splitted1,[0,1,2,n1-1],0)

n2 = splitted2.size

splitted2 = splitted2.tolist()
splitted3 = np.array([])

for i in np.arange(n2):
    splitted2i = splitted2[i]
    splitted3i = splitted2i.split(',')
    splitted3 = np.append(splitted3,splitted3i)
    #This gives a 1D array, code can probably be improved if I make
    #this a 2D array somehow

#The only things we get when output is obs, need to include more/less
#empty lists with different output
#The stuff below just takes the information from splitted3 and divides
#it into the lists depending on type of
#information
#ID of the asteroid, it is - if the asteroid has none
BotId = []
#Name of the asteroid
BotName = []
#RA and Dec of the asteroid at the time of observation in deg
Coords = []
#Class of the asteroid, NEA, main belt, other
Class = []
#Apparent V magnitude of the asteroid at the time of observation
Vmag = np.zeros(n2)
#Error in the position of the asteroid in arcsec
Poserr = np.zeros(n2)

```



```

#Body-to-center angular distance of the asteroid in arcsec
Angsize = np.zeros(n2)
#Motion of the asteroid on the celestial sphere in arcsec/hour
Motion = np.zeros((n2,2))
#Geocentric distance in AU
DBO = np.zeros(n2)
#Heliocentric distance in AU
DBS = np.zeros(n2)
#Phase angle in deg
Alpha = np.zeros(n2)
#Solar elongation in deg
Solelon = np.zeros(n2)

for i in np.arange(n2):
    #amount of values per asteroid (width), dependent on output
    #parameter (output in block 3)
    w = int(splitted3.size/n2)
    BotId.append(splitted3[w*i+0])
    BotName.append(splitted3[w*i+1])
    Coords.append(splitted3[w*i+2]+"_;"+"splitted3[w*i+3])
    Class.append(splitted3[w*i+4])
    Vmag[i] = splitted3[w*i+5]
    Poserr[i] = splitted3[w*i+6]
    Angsize[i] = splitted3[w*i+7]
    Motion[i][0] = splitted3[w*i+8]
    Motion[i][1] = splitted3[w*i+9]
    DBO[i] = splitted3[w*i+10]
    DBS[i] = splitted3[w*i+11]
    Alpha[i] = splitted3[w*i+12]
    Solelon[i] = splitted3[w*i+13]

#Variable that keeps track of the total amount of NEAs in view in a
#field and the detected NEAs as well
NEAsinview = []
NrNEAsinview = []
detNEAlist = np.empty([len(Typelist)], dtype=object)
NrdetNEAlist = np.empty([len(Typelist)], dtype=object)
Appmotinview = []
Appmaginview = np.empty([len(Typelist)], dtype=object)
Vmaginview = []
#Now we need to determine the apparent magnitude for the asteroids
#that are actually NEAs, they have:
#Class = NEA>...
for i in np.arange(n2):

```

```

#Checks if we have a NEA
if Class[i][:4] == 'NEA>':
    NEAsinview.append(BotName[i])
    NrNEAsinview.append(BotId[i])
    #sometimes MPC doesn't have the name of the NEA, so I use try,
    #except
    try:
        NEAindex = Name.index(BotName[i])
        #Below comes all the stuff I want to use from the MPC file,
        #currently only G.
        Gval = float(G[NEAindex])
    except:
        try:
            NEAindex = ID.index((BotId[i]))
            Gval = float(G[NEAindex])
        except:
            #The prints are used so I know that the MPC doesn't
            #have the name of the asteroid
            print("The name: {} was not in the MPC database"
                .format(BotName[i]))
            print(urlopen.in)
            #Below comes the assumed typical values if the name
            #is not in the MPC file
            Gval = 0.15

#Determining the rate of motion of the asteroid from the SkyBot
#information
R = np.sqrt(sum((Motion[i]*24/3600)**2))
Appmotinview.append(R)
#Getting the apparent V band magnitude from the SkyBot
#information
V = Vmag[i]
Vmaginview.append(V)
#Getting the geocentric and heliocentric distance from the
#SkyBot information
dBS = DBS[i]
dBO = DBO[i]
#Getting the phase angle from the SkyBot information
alpha = Alpha[i]
#Sometimes alpha >120, this should result in a very dim asteroid
#and an error, so I might as well set
#it to 120 in that case, since the brightness is not very
#different.
if alpha > 120:

```

```

alpha = 120
#The prints are used so I know that the alpha was too large
print("alpha_is_too_big")
print(urlopen_in)
#List to store the entries of Appmaginview temporary
AppmaginviewT = []
#We can look at the amount of detections when assuming an S-
#and C-type asteroid, the loop goes over
#both
for t in np.arange(len(Typelist)):
    #We can look at the difference that the diameter makes
     #(matters not as explained before)
    #for s,D in enumerate(Dlist): used when I tried to use
    #different diameters (should indent next
    #lines)
    #The two sets of relative albedos for different types
    relPlist = [CrelPlist, S1relPlist, S2relPlist][t]
    #Apparent magnitude using a certain assumed diameter and
    #type for the asteroid in the field
    appmag = vismag(D, relPlist, V, dBS, dBO, Gval, A1, A2, B1, B2, C1, C2
    , alpha)
    #Print can be used for problem solving
    #print(appmag)
    #Including the trailing loss if R >= R0, this makes the
    #apparent magnitude larger
    if R >= R0:
        print("trailing_loss_sets_in")
        appmag += 2.5*np.log10(R/R0)
        #The prints are used so I know when the trailing loss
        #matters
        print(urlopen_in)
        print(appmag)

    #for k,mag in enumerate(appmag): This is not needed for a
    #real observation (going through
    #different bands)
    #n is the index of the band that we are at in the list
    #bandorder
    m = j % 30    #modulus, goes from 0 to 30 on repeat
    #Band we are at
    band = bandorder[m]
    #Index of the band that we are at in the list bandnames
    k = bandnames.index(band)
    #Apparent magnitude of the asteroid with assumed type in

```

```

#the band with index k in the list
#bandnames
mag = appmag[k]
AppmaginviewT.append(mag)
#list that stores the name(s) of the detected NEAs
detNEAs = []
NrdetNEAs = []
#Check to see if the asteroid is detected
if mag <= magmax[k]:
    #Print can be used for problem solving
    #print(D, Typelist[t], bands[k], mag)
    #collecting the names of the detected NEAs
    detNEAs.append(BotName[i])
    NrdetNEAs.append(BotId[i])
#Add the list of detected NEAs to the list that keeps them
#for the different assumptions
if len(detNEAs) > 0:
    detNEAlist[t] = detNEAs
    NrdetNEAlist[t] = NrdetNEAs

#Prints can be used for problem solving
#print(RA[j], Dec[j])
#print(sum(detectarray))
#print(urlopen_in)

#Putting the values of AppmaginviewT in Appmaginview
Appmaginview[0] = AppmaginviewT[0::len(Typelist)]
Appmaginview[1] = AppmaginviewT[1::len(Typelist)]
Appmaginview[2] = AppmaginviewT[2::len(Typelist)]

#n is the index of the band that we are at in the list bandorder
m = j % 30    #modulus, goes from 0 to 30 on repeat
#Band we are at
band = bandorder[m]

#I don't want the file to show empty lists, so I change an empty list
#to None
if len(NEAsinview) == 0 :
    NEAsinview = None
    NrNEAsinview = None
    Appmotinview = None
    Vmaginview = None

```



```
    print()  
    pass  
  
time.sleep(60)
```

References

- Blackgem telescope array. Online, a. Accessed 27-06-2019 URL: https://docs.wixstatic.com/ugd/4ab709_0b1fddbe73ca406e97aafb75904936b3.pdf.
- Blackgem. Online, b. Accessed 7-06-2019 URL: <https://astro.ru.nl/blackgem/>.
- Ceres: Keeping well-guarded secrets for 215 years. Online. Accessed 24-06-2019 URL: <https://www.jpl.nasa.gov/news/news.php?feature=4824>.
- Groningen monthly climate averages. Online. Accessed 24-06-2019 URL: <https://www.worldweatheronline.com/groningen-weather-averages/groningen/nl.aspx>.
- General observing conditions and data for la silla. Online. Accessed 24-06-2019 URL: <http://www.eso.org/gen-fac/pubs/astclim/lasilla/index.html>.
- Notes from the iau general assembly. Online. Accessed 3-07-2019 URL: https://minorplanetcenter.net/iau/ECS/MPCArchive/1985/MPC_19851227.pdf.
- Discovery statistics. Online. Accessed 3-07-2019 URL: https://cneos.jpl.nasa.gov/stats/site_all.html.
- Neo basics. Online. Accessed 5-06-2019 URL: https://cneos.jpl.nasa.gov/about/neo_groups.html.
- H. rept. 109-158 - george e. brown, jr. near-earth object survey act. Online. Accessed 26-06-2019 URL: <https://www.congress.gov/congressional-report/109th-congress/house-report/158/1>.
- J. Berthier, F. Vachier, W. Thuillot, P. Fernique, F. Ochsenbein, F. Genova, V. Lainey, and J.-E. Arlot. SkyBoT, a new VO service to identify Solar System objects. In C. Gabriel, C. Arviset, D. Ponz, and S. Enrique, editors, *Astronomical Data Analysis Software and Systems XV*, volume 351 of *Astronomical Society of the Pacific Conference Series*, pages 367–+, July 2006.
- Audrey Bouvier and Meenakshi Wadhwa. The age of the Solar System redefined by the oldest Pb-Pb age of a meteoritic inclusion. *Nature Geoscience*, 3(9):637–641, Sep 2010. doi: 10.1038/ngeo941.
- Imke de Pater and Jack J. Lissauer. *Planetary Sciences*. Cambridge University Press, 2015.
- A. W. Harris and G. D’Abramo. The population of near-Earth asteroids. *Icarus*, 257: 302–312, September 2015. doi: 10.1016/j.icarus.2015.05.004.
- Željko Ivezić, Serge Tabachnik, Roman Rafikov, Robert H. Lupton, Tom Quinn, Mark Hammergren, Laurent Eyer, Jennifer Chu, John C. Armstrong, Xiaohui Fan, Kristian Finlator, Tom R. Geballe, James E. Gunn, Gregory S. Hennessy, Gillian R. Knapp, Sandy K. Leggett, Jeffrey A. Munn, Jeffrey R. Pier, Constance M. Rockosi, Donald P. Schneider, Michael A. Strauss, Brian Yanny, Jonathan Brinkmann, István Csabai, Robert B. Hindley, Stephen Kent, Don Q. Lamb, Bruce Margon, Timothy A. McKay, J. Allyn Smith,

- Patrick Waddell, and Donald G. York. Solar system objects observed in the sloan digital sky survey commissioning data. *The Astronomical Journal*, 122(5):2749–2784, nov 2001. doi: 10.1086/323452. URL <https://doi.org/10.1086%2F323452>.
- R. Jedicke, M. Granvik, M. Micheli, E. Ryan, Spahr T., and D. K. Yeomans. Surveys, Astrometric Follow-up & Population Statistics. In P. Michel, F. DeMeo, and W. Bottke, editors, *ASTEROIDS IV*. University of Arizona Press, March 2015.
- C.-I Lagerkvist and Iwan Williams. Physical studies of asteroids. xv - determination of slope parameters and absolute magnitudes for 51 asteroids. *Astronomy and Astrophysics Supplement Series*, 68:295–315, 02 1987.
- LSST Science Collaboration, Paul A. Abell, Julius Allison, Scott F. Anderson, John R. Andrew, J. Roger P. Angel, Lee Armus, David Arnett, S. J. Asztalos, and Tim S. Axelrod. LSST Science Book, Version 2.0. *arXiv e-prints*, art. arXiv:0912.0201, Dec 2009.
- A. Mainzer, J. Bauer, T. Grav, J. Masiero, R. M. Cutri, J. Dailey, P. Eisenhardt, R. S. McMillan, E. Wright, and R. Walker. Preliminary Results from NEOWISE: An Enhancement to the Wide-field Infrared Survey Explorer for Solar System Science. *The Astrophysical Journal*, 731(1):53, Apr 2011. doi: 10.1088/0004-637X/731/1/53.
- Nicholas Moskovitz and Eric Gaidos. Differentiation of planetesimals and the thermal consequences of melt migration. *Meteoritics and Planetary Science*, 46(6):903–918, Jun 2011. doi: 10.1111/j.1945-5100.2011.01201.x.
- Peter Vereš, Robert Jedicke, Richard Wainscoat, Mikael Granvik, Steve Chesley, Shinsuke Abe, Larry Denneau, and Tommy Grav. Detection of Earth-impacting asteroids with the next generation all-sky surveys. *Icarus*, 203(2):472–485, Oct 2009. doi: 10.1016/j.icarus.2009.05.010.